Item 830-H-15 NAS 1.60:1207

SEP 6 1978

NASA Technical Paper 1207

COMPLETED
ORIGINAL

Turbulent-Flow Separation Criteria for Overexpanded Supersonic Nozzles

E. Leon Morrisette and Theodore J. Goldberg

AUGUST 1978

NASA

(39)

Item 830-H-15 NAS 1.60:1207

NASA Technical Paper 1207

Turbulent-Flow Separation Criteria for Overexpanded Supersonic Nozzles

E. Leon Morrisette and Theodore J. Goldberg
Langley Research Center
Hampton, Virginia

National Aeronautics
and Space Administration

**Scientific and Technical
Information Office**

1978

SUMMARY

A comprehensive compilation of available turbulent-flow separation data for over-expanded supersonic nozzles is presented with a discussion of correlation techniques and prediction methods. Data are grouped by nozzle types: conical, contoured, and two-dimensional wedge. Correlation of conical-nozzle separation is found to be independent of nozzle divergence half-angle above about 9°, whereas the contoured-nozzle data follow a different correlation curve. Zero-pressure-gradient prediction techniques are shown to predict adequately the higher divergence-angle conical separation data, and an empirical equation is given for the contoured-nozzle data correlation. Flow conditions for which the correlations are invalid are discussed and bounded. A nozzle boundary-layer transition criterion is presented which can be used to show that much of the noncorrelating data in the literature are concerned with nonturbulent separation and which explains the previously reported "external flow effects" on nozzle separation.

INTRODUCTION

The flow field of a supersonic nozzle exhausting to an ambient pressure greater than that for which the nozzle is designed will contain oblique shock waves, and the flow may separate from the walls as a supersonic jet which fills only a portion of the cross-sectional area available for expansion. This realistic behavior is in contrast to the theoretical inviscid description (ref. 1) of supersonic expansion after the throat, followed by a normal shock and subsonic compression. This is the classical flow pattern that would exist if there were no boundary layer. Figure 1 illustrates the difference between the two cases.

For the case with separation, the nozzle flow expands from the supply pressure p_t to a minimum wall static pressure, usually designated in nozzle-separation studies as the separation pressure p_s. Separation occurs upstream of where a normal shock would occur and, when the flow separates, the pressure rises to ambient pressure much more rapidly than the pressure rise associated with subsonic compression. This results in higher wall pressures for the separated case and improved performance (higher thrust) over the normal shock case. For vehicles such as proposed hypersonic research aircraft which have afterbodies that act as the nozzle, separation location will affect lift and stability characteristics as well as thrust. Obviously, knowledge of the point of separation is essential for performance prediction. Studies have been made (refs. 2 to 4) of techniques to induce and control separation for both improved stability and performance.

Nozzles for launch vehicles are usually designed for some average expansion ratio which would give the best overall performance through the full trajectory. Thus, the nozzle will be operating at an off-design overexpanded condition at lower altitudes and will be susceptible to separation.

The present paper presents a comprehensive review of available supersonic-nozzle separation data. A review of correlation and prediction techniques is made, and predictions are compared with the separation characteristics for various types of supersonic nozzles. It is shown that much of the scatter in separation pressure ratios at low Mach numbers is due to the existence of laminar or transitional flow which also explains the difference in data taken with and without an external coflowing stream. An appendix is included which gives an example of the application of the correlation techniques to a typical nozzle.

SYMBOLS

A	cross-sectional area of nozzle
A^*	cross-sectional area of nozzle at throat
f	function
M	Mach number
M_1	Mach number ahead of separation shock
M_2	Mach number behind separation shock
p	pressure
R_{tr}	transition Reynolds number
R_x	Reynolds number based on length along nozzle from throat
R^*	Reynolds number based on throat (sonic) conditions and throat diameter
u_s	velocity at boundary-layer edge
u_s^*	characteristic velocity in boundary layer (ref. 31)

ICE, NA

x	spatial coordinate along nozzle axis with origin at throat
α	half-angle of conical nozzle or local wall angle for other nozzles (see fig. 1)
γ	specific heat ratio

Subscripts:

a	external ambient conditions at nozzle exit
e	exit
ext	conditions in external coflowing stream at nozzle exit
s	undisturbed value just ahead of separation (see fig. 1)
t	total conditions in stagnation chamber
w	wall conditions

REVIEW OF SUPERSONIC-NOZZLE SEPARATION DATA

History

Separation in nozzles was first noticed in the early 1900's as steam turbines came into use; however, no criteria were established for the prediction of the onset of separation. Detailed investigations did not appear until the advent of rocket propulsion in the late 1940's when nozzle flow separation became a matter of practical importance. Some of the first quantitative correlations related separation in conical and two-dimensional nozzles to settling-chamber pressure p_t (ref. 5). Most of these studies showed that the separation pressure ratio (ratio of the nozzle wall pressure just upstream of separation to the external ambient pressure p_s/p_a) was independent of design expansion ratio, nozzle divergence angle, ratio of specific heats, and gas temperature; as a consequence, a value of $p_s/p_a = 0.4$ was used as a separation criteria and is still quoted today (e.g., see ref. 6) although more recent studies have shown it to be inadequate. The results of Scheller and Bierlein (ref. 7) conflicted with the other early investigations in that they found the separation pressure to be dependent on nozzle divergence angle. They also suggested that Reynolds number might be an important correlation parameter, but the lack of available data at that time prevented any correlation. Meleney and Kuhns (ref. 8) reported that as separation location approached the throat, the separation pressure ratio was more influenced by the ambient pressure. Considerable experimental work has been

devoted to nozzle separation. The reported investigations are too numerous to mention individually, but references 9 to 49 in addition to those previously mentioned are examples of the work done to determine the effects of various parameters on separation in supersonic nozzles.

Correlation Parameters

A number of correlations have been suggested by various investigators. Early workers in the field used

$$\frac{p_t}{p_a} = f\left(\frac{A_s}{A^*}\right) \tag{1}$$

and

$$\frac{p_s}{p_t} = f\left(\frac{p_t}{p_a}\right) \tag{2}$$

Green (ref. 13) suggested a modification of equation (2):

$$\frac{p_a}{p_t} - \frac{p_s}{p_t} = f\left(\frac{p_a}{p_t}\right) \tag{3}$$

which through the use of the redundant parameter p_a/p_t resulted in apparent suppression of scatter. However, this reduction in scatter was actually accomplished through a conversion to a higher reference value.

More recent investigations have suggested

$$\frac{p_s}{p_a} = f\left(\frac{p_t}{p_a}\right) \tag{4}$$

and

$$\frac{p_s}{p_a} = f(M_s) \tag{5}$$

Although the first of these equations (eq. (4)) has the merit of being written in more convenient terms for the designer, with p_t being a function of engine design and p_a a function of flight environment, the second equation (eq. (5)) is more closely related to the local conditions at boundary-layer separation and is used in the present paper. Lawrence (ref. 42) achieved better correlation with equation (5) than with equation (4) and suggested it to be the preferable correlation. The two equations are actually related through the isentropic relation

$$M_s = f\left(\frac{p_s}{p_t}, \gamma\right) \tag{6}$$

with γ having only a small effect at lower Mach numbers where data are available for a range of γ. It will later be shown that the effect of γ is not apparent from the available data.

Prediction Methods

A number of predictions and correlations of the separation pressure ratio for turbulent boundary layers are shown in figure 2. Also shown is the pressure ratio across a normal shock wave. In general, shock-separated boundary layers are classified in two groups: free and restricted separations. Chapman, Kuehn, and Larson (ref. 50) refer to the first of these as a free-interaction separation and define it as a separation which is not directly influenced by downstream geometry. Separation in overexpanded nozzles of wide divergence is an example of free-interaction separation since there is no reattachment to the nozzle and no required separated-flow direction.

Reshotko and Tucker (ref. 51) developed a semianalytical prediction method for the onset of turbulent separation. In this method, empirical incompressible separation criteria are used in conjunction with a compressibility transformation to predict separation for the compressible case. A relationship between the local Mach number and velocity profile (form factor) provides a means of determining a Mach number ratio across the discontinuity for shock-induced separation. The Mach number ratio was found to be 0.762 for zero-pressure-gradient flows and somewhat lower for favorable pressure-gradient flows. Calculations of p_s/p_a as a function of M_s are shown in figure 2 for this method using the Mach number ratio of 0.762 with $\gamma = 1.2$ and 1.4. This technique and its application to separation in nozzles are discussed more fully in Lawrence's thesis (ref. 42).

Arens and Spiegler (ref. 34) utilized the assumption, first suggested by Gadd (ref. 52), that the pressure rise associated with separation must be sufficient to stagnate a characteristic velocity in the boundary layer u_s^*. This theory is also shown in figure 2 for a value of $u_s^*/u_s = 0.6$ (as suggested in ref. 34) where u_s is the local velocity at the edge of the boundary layer at separation. Reference 34 points out that this theory (as well as all others shown herein) assumes the separation peak pressure to be equal to the ambient exhaust pressure and does not account for any compression associated with the mixing region downstream of separation.

Also shown in figure 2 are the empirical curves representing the zero-pressure-gradient flat-plate data of Chapman, Kuehn, and Larson (ref. 50) and Sterrett and Emery (ref. 53) for incipient separation. Reference 50 observed a slight Reynolds number effect on the separation pressure ratio, and the curve shown represents data for a Reynolds number of 10^6. Reference 53 did not show an effect of Reynolds number and Holden

(ref. 54) showed the effect of Reynolds number to be on the order of $R_x^{-1/10}$ at higher Reynolds numbers (above 10^6). The pressure rise associated with a normal shock as well as the theory of Reshotko and Tucker (ref. 51) is shown (see fig. 2) for comparison on all subsequent correlation plots of p_s/p_a as a function of separation Mach number.

CORRELATION OF SEPARATION DATA FOR SUPERSONIC NOZZLES

Factors Causing Data Scatter

Transition effects.- Some typical examples of nozzle-separation data are correlated in figure 3 in terms of p_s/p_a as a function of M_s. The data of Meleney and Kuhns (ref. 8) show a wide variation in separation pressure ratio at low Mach numbers (see fig. 3(a)), typical of the scatter found in the literature. It is assumed by the present authors that the data for the low ambient pressure (0.33 atm or 33.43 kPa in fig. 3(a)) below $M_s = 2.4$ are for laminar or transitional separation. The data of Herbert and Martlew (ref. 38) are reported to be laminar for the smooth-wall case and to be tripped by roughness ahead of the throat for the turbulent case (noted as rough-wall data in fig. 3(b)).

In order to reduce the scatter in data correlations, especially at the low Mach numbers, an attempt was made to define a boundary between laminar and turbulent separation by utilizing the data of Meleney and Kuhns (ref. 8). This was done by cross-plotting the data to allow the separation pressure ratio to be determined as a function of Reynolds number for constant values of separation Mach number M_s. Two Reynolds numbers were calculated: the first was a length Reynolds number R_x, based on free-stream conditions at the point of separation and axial distance from the throat; the second was a throat Reynolds number R^*, based on sonic flow conditions and the throat diameter. Some authors have suggested R^* as a characteristic of nozzles (ref. 37).

The separation pressure ratios as a function of each of these Reynolds numbers are shown in figure 4. The data for each separation Mach number are characterized by a region of only small changes in separation pressure ratio until some lower value of Reynolds number is reached and the separation pressure ratio suddenly increases. This sudden break in the curve is believed to be the demarcation between laminar and transitional separation. The Reynolds number at this point of sudden increase is shown in figure 5 against separation Mach number and is defined as a transition Reynolds number. Data falling below these curves are considered to be cases of laminar separation. Although this criterion is based on only one set of data, it does eliminate much of the scatter in the correlation of data as will be subsequently seen. This criterion is applied to nozzles of widely differing shape since there are not enough data to establish the effect of geometry on the transition Reynolds numbers. Reference 8 does not distinguish

between the data as laminar or turbulent but simply refers to the low Mach number variation in the separation pressure ratio as being "influenced to a greater extent by the discharge pressure p_a." By the reasoning given herein, it is felt that the supply pressure p_t is the primary influence since it determines the Reynolds number.

Nozzle-exit effects.- The data of figure 3(b) show another feature of nozzle separation which has increased data scatter in proposed correlations. Separation near the nozzle exit causes the separation pressure ratio to rise above the normal downward trend with increasing M_s. This region of increasing p_s/p_a is small for the turbulent data and somewhat larger for the laminar data. In an effort to correlate the location in the nozzle at which the ratio p_s/p_a increases above the expected trend, the nozzle pressure ratio p_t/p_s and separation Mach number at which "exit deviation" occurs from the correlation of p_s/p_a against M_s are shown as a function of nozzle-design pressure ratio p_t/p_e and design exit Mach number in figure 6. There is scatter in the data but the curve given by

$$\frac{A_s}{A^*} = 0.8\,\frac{A_e}{A^*} \tag{7}$$

often suggested in the literature (ref. 40) seems to be a reasonable guide above a Mach number of 2. A modification of equation (7) given as

$$\frac{A_s}{A^*} = 0.8\left(\frac{A_e}{A^*} - 1\right) + 1 \tag{8}$$

seems to fit the data better at low exit Mach numbers. Data falling below this curve should follow the correlation of p_s/p_a plotted against M_s.

Also indicated in figure 3(b) are example values for which an oblique shock exists at the nozzle exit without separation occurring ($M_s = M_e$). The limiting overall nozzle pressure ratio p_t/p_a for this condition is shown in figure 7 as a function of design pressure ratio. These data can be well represented by the curve (ref. 19) given by

$$\frac{p_t}{p_a} = 1 + 0.39\,\frac{p_t}{p_e} \tag{9}$$

Pressure ratios p_t/p_a above this curve will not separate the flow.

Correlations of Experimental Data

The available values of separation pressure ratios for nozzles are shown in figures 8 to 11 as a function of separation Mach number. Experimental data are included for conical and contoured, two-dimensional, and axisymmetric nozzles exhausting into still air and with a coflowing external stream. Data which showed the exit deviation

noted earlier in the discussion of figures 3(b) and 6 are omitted from figures 8 to 11. Data for which Reynolds numbers could be calculated and which fell below the transition Reynolds number curves of figure 5 are shown as solid symbols. For much of the available data (see table I) there is not sufficient information to calculate the Reynolds numbers.

Conical nozzles.- Separation pressure ratios for conical nozzles with low divergence angles shown in figure 8(a) are seen to be in fair agreement with the theory of Reshotko and Tucker (ref. 51) only around a Mach number of 2 and to fall considerably below the theory at higher separation Mach numbers. The data of figure 8(b) for slightly higher values of nozzle divergence more closely approach the theory throughout the separation Mach number range above $M_s = 1.7$. The turbulent data for all higher divergence angles (figs. 8(c) and (d)) closely agree with the theory above $M_s = 1.7$. Below $M_s = 1.7$ the data for all divergence angles fall below the theory, thus showing a tendency to level off at a value of p_s/p_a between 0.5 and 0.6. There may be a stronger Reynolds number effect in this region where, in general, the Reynolds numbers are very low. Figure 4 shows some variation of separation pressure ratio with Reynolds number even for the turbulent data. This deviation from the theory may also be a result of the very strong pressure gradient close to the throat of the nozzle. As was indicated earlier, a lower value of the Mach number ratio used in the Reshotko and Tucker theory (ref. 51) was suggested for favorable pressure-gradient flows. Mager (ref. 55) also indicates that the ratio should decrease slightly at lower Mach numbers.

Note that a few data points show a pressure rise at separation greater than that for a normal shock loss. (In figs. 3(a) and (b), p_s/p_a is smaller than normal shock values.) This occurs because the entire pressure rise is not obtained at the point of separation. If a normal shock exists at the separation point for the data below the normal-shock pressure-rise curve, the flow then diffuses subsonically to the ambient exhaust pressure. (See fig. 1(b).)

The data of figures 8(b) to (d) have specific heat ratios of 1.2 to 1.4 (see table I), but no effect of specific heat ratio on separation pressure ratio is discernible in the data. The theories of Arens and Spiegler (ref. 31) and of Reshotko and Tucker (ref. 51) show an increasing effect of specific heat ratio on the separation pressure ratio as Mach number increases (fig. 2). The available data having a specific heat ratio of other than 1.4 are limited to data below $M_s = 3.2$, and a specific-heat-ratio effect may be masked by the data scatter.

Two-dimensional wedge nozzles.- Separation pressure ratios for two-dimensional wedge-flow nozzles (fig. 9) correlate similarly as those for conical nozzles. The cause of the rise in the separation pressure ratio above $M_s = 3.1$ for McKenney's data (ref. 11) is not known but it is not a low Reynolds number effect. Much of the scatter in the data

below $M_s = 2$ may be due to low turbulent Reynolds numbers or laminar flow; however, the Reynolds numbers are not available for the data of reference 31.

Axisymmetrical contoured nozzles.- The data for contoured nozzles (fig. 10), the case of most interest for modern nozzle design, fall below the prediction of Reshotko and Tucker (ref. 51) at separation Mach numbers greater than about 3. A similar trend was found with low-divergence-angle conical nozzles (fig. 8(a)) which is not surprising since both types of nozzles have low local wall angles above $M_s = 3$ (near the exit for contoured nozzles). The close proximity of the wall may eliminate these cases from the free-interaction separation category discussed earlier. Lawrence (ref. 42) and Guman (ref. 56) suggest that the close proximity of the wall to the shear layer (see fig. 1(a)) causes a change in the entrainment process and that the pressure rise is the pressure necessary to drive the reverse-flow entrainment air in the narrow region between the wall and the mixing region. Lawrence also showed that using the pressure plateau just downstream of separation in place of p_a resulted in agreement with theory. Guman (ref. 56) suggested the use of a percentage of p_a (65 percent) as a correlating parameter but this would probably vary with each case. A knowledge of the entrainment process is necessary for a prediction technique to be applied.

An empirical equation is shown in figure 10 which is a second-order curve fit to the data (other than ref. 33) between $M_s = 2.4$ and $M_s = 4.5$. This equation is

$$\frac{p_s}{p_a} = 1.082 - 0.363M_s + 0.0386M_s^2 \tag{10}$$

The data of Roschke and Massier (ref. 33) deviate rapidly upward above $M_s = 3.4$ and are never in close agreement with the rest of the data. Although the Reynolds numbers are not available for these data, it is noted in reference 33 that the rapidly rising data were obtained at low back pressures, which indicates lower supply pressures p_t for the same overall pressure ratios. Thus, the flow may have been laminar at these lower supply pressures. (See fig. 3(a).)

Nozzles with external coflowing stream.- Several studies have been made of nozzles exhausting into coflowing external flows. The first of these (ref. 15) indicates that for supersonic external streams the flow separates at much lower back pressures (higher p_s/p_a) than with quiescent external air. These data are shown in figure 11 along with the data of references 22, 27, and 37, which would agree with the conclusion of reference 15 until the Reynolds numbers are examined. Elimination of the laminar points and the data of reference 15, for which Reynolds numbers are not available, gives results which follow a trend similar to that of the higher divergence-angle conical nozzles.

Comparison of data for various nozzles.- A summary of the data of figures 8 to 11 is shown in figure 12. Here it can be clearly seen that the correlation of Reshotko and Tucker (ref. 51) is valid for the high-divergence-angle conical nozzles and is invalid for the low-divergence-angle conical nozzles and contoured nozzles at higher separation Mach numbers. Also shown is the empirical equation (eq. (10)) for the contoured nozzles. The appendix gives an example of the application of the correlation techniques to a typical nozzle.

CONCLUSIONS

An analysis of available experimental data on turbulent-flow separation in overexpanded supersonic nozzles resulted in the following conclusions:

1. The data can be correlated for each type of nozzle if data near the nozzle exit are excluded and if laminar data are distinguished and eliminated.

2. Separation in nozzles can be predicted by using zero-pressure-gradient free-interaction theory over most of the nozzle length for wall divergence angles greater than about 10°.

3. Prediction of separation for low-divergence-angle conical nozzles and for the low wall-angle region of contoured nozzles requires knowledge of the pressure rise in the entrainment process and is no longer a free-interaction separation.

4. No obvious effect of specific heat ratio was found when the data were correlated in the form of separation pressure ratio as a function of separation Mach number.

Langley Research Center
National Aeronautics and Space Administration
Hampton, VA 23665
May 31, 1978

APPENDIX

EXAMPLE OF USE OF CORRELATION

A sample of the procedure for determining the separation point in a particular nozzle at certain flow conditions is presented in this appendix. Figure A1 is a sketch of a typical conical nozzle having a 15° half-angle and an exit-to-throat area ratio of 8.125. The linear dimensions of the nozzle are not needed in applying the separation criterion if the flow is known to be turbulent. If not known to be turbulent, the length or throat Reynolds numbers may be calculated for comparison with the transition criterion of figure 5.

Figure A2 gives the calculated pressure distribution for the nozzle if assuming one-dimensional flow and a specific heat ratio equal to 1.4. By using the theory of Reshetko and Tucker (ref. 51) which was a good fit to the 15° conical-nozzle data of figure 8(c) (other empirical fairings of data or theories could be used), the values of p_s/p_a are determined for various Mach numbers along the nozzle at various x-positions. The separation Mach number is simply the wall Mach number immediately ahead of separation and is a function of the nozzle design. The value of p_s/p_a at each x-position divided by the corresponding value of p_w/p_t (fig. A2) gives the desired ratio of nozzle total pressure (a design parameter) to ambient pressure (a function of flight environment). The resulting curve of separation location as a function of p_t/p_a is shown in figure A3. The position downstream of which the correlation no longer holds (from fig. 6) is indicated near the exit as point A, and the value of p_t/p_a (from fig. 7) above which separation will not occur is indicated at the exit as point B. A straight-line fairing between the two values is shown but the actual curve may differ somewhat.

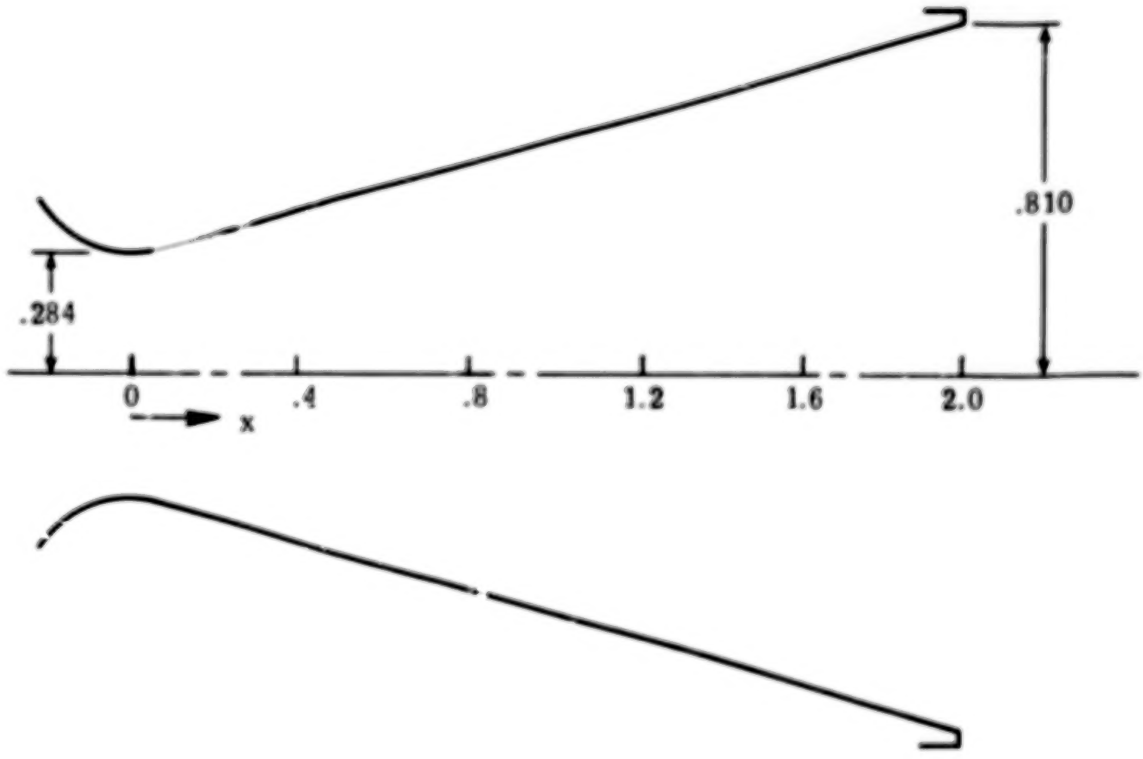

Figure A1.- Typical conical nozzle with 15° half-angle and exit-to-throat area ratio of 8.125.

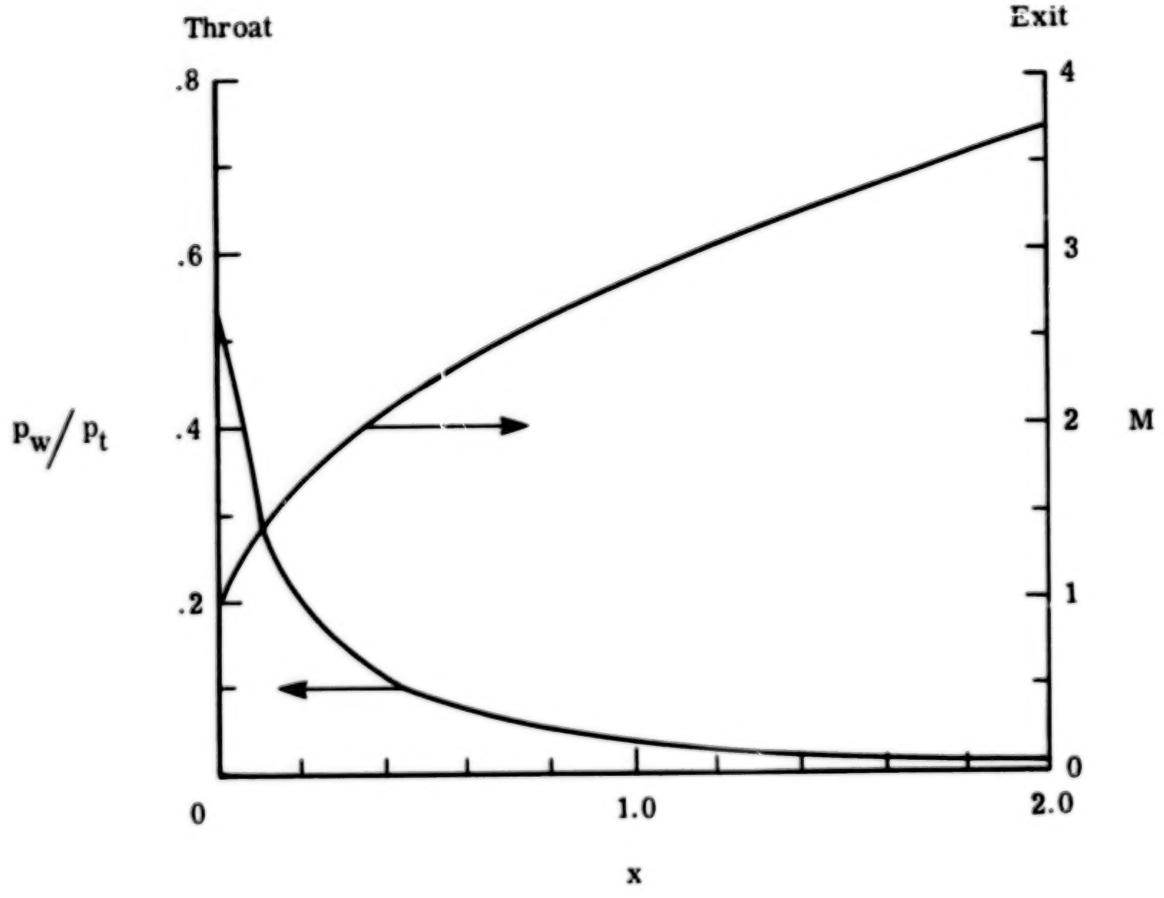

Figure A2.- Mach number and pressure distribution of nozzle.

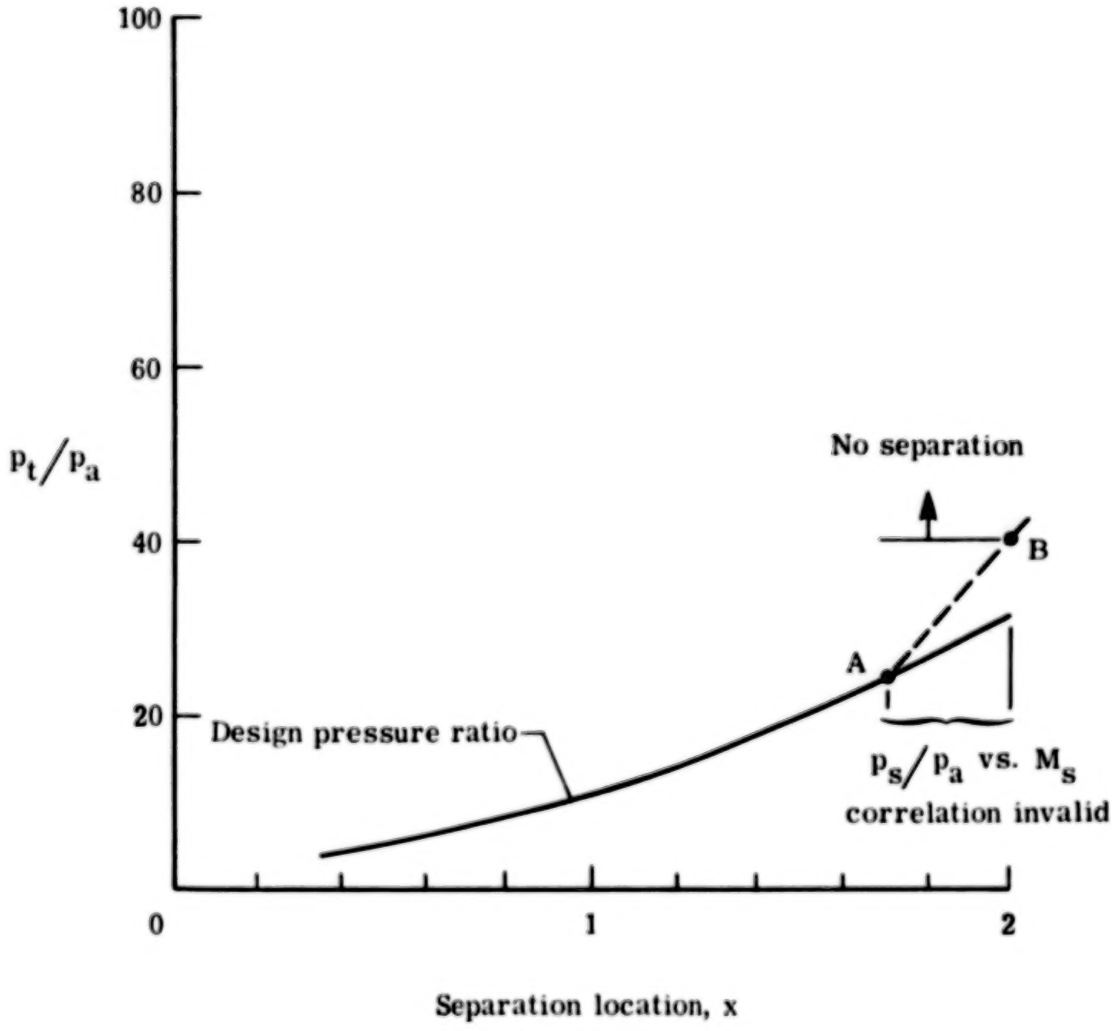

Figure A3.- Separation location as a function of overall pressure ratio p_t/p_a.

REFERENCES

1. Malina, Frank J.: Characteristics of the Rocket Motor Unit Based on the Theory of Perfect Gases. J. Franklin Inst., vol. 230, no. 4, Oct. 1940, pp. 433-454.

2. Green, L., Jr.; and Nall, K. L.: Control of Flow Separation in Supersonic Nozzles by Means of Boundary-Layer Injection. Spec. Rep. 1381 (Contract No. AF-33(616)-3767), Aerojet-General Corp., Dec. 31, 1957.

3. Schmucker, R. H.: A Procedure for Calculation of Boundary Layer Trip Protuberances in Overexpanded Rocket Nozzles. NASA TM X-64843, 1973.

4. Rowe, J. R.; and Berner, F.: An Investigation of Controlled Flow Separation in Nozzles. Spec. Rep. No. 1205, Aerojet-General Corp., Dec. 19, 1956.

5. Foster, Charles R.; and Cowles, Frederick P.: Experimental Study of Gas-Flow Separation in Overexpanded Exhaust Nozzles for Rocket Motors. Progress Rep. No. 4-103 (Contract No. W-04-200-ORD-455, Ord. Dept.), Jet Propul. Lab., California Inst. Technol., May 9, 1949.

6. Sutton, George P.; and Ross, Donald M.: Rocket Propulsion Elements – An Introduction to the Engineering of Rockets. Fourth ed. John Wiley & Sons, Inc., c.1976.

7. Scheller, Karl; and Bierlein, James A.: Notes on Flow Separation in Rocket Nozzles. Air Materiel Command, U.S. Air Force, 1950.

8. Meleney, R. H.; and Kuhns, R. M.: Flow Separation in Over-Expanded Supersonic Nozzles. Rt-115, Consolidated Vultee Aircraft Corp., Oct. 23, 1951.

9. Foster, Charles R.; and Cowles, Frederick B.: Experimental Determination of the Static-Pressure Distribution in an Overexpanded Rocket-Motor Exhaust Nozzle. Progress Rep. No. 4-125 (Contract No. W-04-200-ORD-455), Jet Propul. Lab., California Inst. of Technol., Mar. 21, 1950.

10. Foster, Charles R.; and Cowles, Frederick B.: Experimental Study of the Divergence-Angle Effect in Rocket-Motor Exhaust Nozzles. Progress Rep. No. 20-134 (Contract No. DA-04-495-Ord 18), Jet Propul. Lab., California Inst. Technol., Jan. 16, 1951.

11. McKenney, John D.: An Investigation of Flow Separation in a Two-Dimensional Transparent Nozzle. Progress Rep. No. 20-129 (Contract No. DA-04-495-Ord 18), Jet Propul. Lab., California Inst. Technol., Apr. 4, 1951.

12. Krull, H. George; and Steffen, Fred W.: Performance Characteristics of One Convergent and Three Convergent-Divergent Nozzles. NACA RM E52H12, 1952.

13. Green, Leon, Jr.: Flow Separation in Rocket Nozzles. J. American Rocket Soc., vol. 23, no. 1, Jan.-Feb. 1953, pp. 34-35.

14. Scheller, Karl; and Bierlein, James A.: Some Experiments on Flow Separation in Rocket Nozzles. J. American Rocket Soc., vol. 23, no. 1, Jan.-Feb. 1953, pp. 28-32, 40.

15. Fradenburgh, Evan A.; Gorton, Gerald C.; and Beke, Andrew: Thrust Characteristics of a Series of Convergent-Divergent Exhaust Nozzles at Subsonic and Supersonic Flight Speeds. NACA RM E53L23, 1954.

16. Summerfield, Martin; Foster, Charles R.; and Swan, Walter C.: Flow Separation in Overexpanded Supersonic Exhaust Nozzles. Jet Propul., vol. 24, no. 5, Sept.-Oct. 1954, pp. 319-321.

17. Steffen, Fred W.; Krull, H. George; and Schmiedlin, Ralph F.: Effect of Divergence Angle on the Internal Performance Characteristics of Several Conical Convergent-Divergent Nozzles. NACA RM E54H25, 1954.

18. Eisenklam, P.; and Wilkie, D.: On Jet Separation in Supersonic Rocket Nozzles. I – The Characteristics of Flow. D.G.G.W. Rep. EMR/55/4 (Imperial Coll. Rep. J.R.L. No. 29), British Minist. Supply, May 1955.

19. Ashwood, P. F.; and Crosse, G. W.: The Influence of Pressure Ratio and Divergence Angle on the Shock Position in Two-Dimensional, Over-Expanded, Convergent-Divergent Nozzles. C.P. No. 327, British A.R.C., 1957.

20. Ionov, V. P.: Supersonic Flow at Different Reynolds Numbers in Contoured Nozzles Under Conditions of Overexpansion. NASA TT F-79, Israel Program Sci. Transl., c.1962, pp. 82-84. (Available from NTIS, U.S. Dep. Com.)

21. Fraser, R. P.; Eisenklam, Paul; and Wilkie, D.: Investigation of Supersonic Flow Separation in Nozzles. J. Mech. Eng. Sci., vol. 1, no. 3, 1959, pp. 267-279.

22. Musial, Norman T.; and Ward, James J.: Overexpanded Performance of Conical Nozzles With Area Ratios of 6 and 9 With and Without Supersonic External Flow. NASA TM X-83, 1959.

23. Schueller, Carl F.: Interactions Between the External Flow and Rocket Exhaust Nozzle. Paper No. 59-133, Inst. Aeronautical Sci., 1959.

24. Campbell, C. E.; and Farley, J. M.: Performance of Several Conical Convergent-Divergent Rocket-Type Exhaust Nozzles. NASA TN D-467, 1960.

25. Farley, John M.; and Campbell, Carl E.: Performance of Several Method-of-Characteristics Exhaust Nozzles. NASA TN D-293, 1960.

26. Lamb, Jamie Parker, Jr.: A Study of Flow Separation in Overexpanded, Conical, Convergent-Divergent Nozzles. Ph. D. Thesis, Univ. of Illinois, 1961.

27. Reid, J.; and Hastings, R. C.: The Effect of a Central Jet on the Base Pressure of a Cylindrical After-Body in a Supersonic Stream. R. & M. No. 3224, British A.R.C., 1961.

28. Ahlberg, J. H.; Hamilton, S.; Migdal, D.; and Nilson, E. N.: Truncated Perfect Nozzles in Optimum Nozzle Design. A.R.S. J., vol. 31, no. 5, May 1961, pp. 614-620.

29. Bloomer, Harry E.; Antle, Robert J.; and Renas, Paul E.: Experimental Study of Effects of Geometric Variables on Performance of Conical Rocket-Engine Exhaust Nozzles. NASA TN D-846, 1961.

30. Bloomer, Harry E.; Antl, Robert J.; and Renas, Paul E.: Experimental Study of Effects of Geometric Variables on Performance of Contoured Rocket-Engine Exhaust Nozzles. NASA TN D-1181, 1962.

31. Arens, M.; and Spiegler, E.: Separated Flow in Overexpanded Nozzles at Low Pressure Ratios. Bull. Res. Counc. of Israel, vol. 11C, no. 1, Apr. 1962, pp. 45-55.

32. Arens, M.: Turbulent Shock-Wave Boundary Layer Separation and Overexpanded Nozzle Flow. Proceedings of the XIIIth International Astronautical Congress. N. Boneff and I. Hersey, eds., Springer-Verlag, 1964, pp. 788-799.

33. Roschke, E. J.; and Massier, P. F.: Flow Separation in a Contour Nozzle. ARS J., vol. 32, no. 10, Oct. 1962, pp. 1612-1613.

34. Arens, M.; and Spiegler, E.: Shock-Induced Boundary Layer Separation in Overexpanded Conical Exhaust Nozzles. AIAA J., vol. 1, no. 3, Mar. 1963, pp. 578-581.

35. Arens, M.: The Shock Position in Overexpanded Nozzles. J. R. Aeronaut. Soc., vol. 67, no. 628, Apr. 1963, pp. 268-269.

36. Arens, M.: Flow Separation in Overexpanded Contoured Nozzles. AIAA J., vol. 1, no. 8, Aug. 1963, pp. 1945-1946.

37. Golesworthy, G. T.; and Herbert, M. V.: The Performance of a Conical Convergent-Divergent Nozzle With Area Ratio 2.9 in External Flow. C.P. No. 891, British A.R.C., Nov. 1963.

38. Herbert, M. V.; and Martlew, D. L.: A Digest of Report No. R.258 Entitled "The Design-Point Performance of Model Internal-Expansion Propelling Nozzles With Area Ratios Up to 4." N.G.T.E. Rep. No. R.258a, British Minist. Avia., Apr. 1964.

39. Moore, Clifford James, Jr.: An Experimental Study of Flow Separation and Instability in an Overexpanded Nozzle. M.S. Thesis, Southern Methodist Univ., Jan. 28, 1964.

40. Sunley, H. L. G.; and Ferriman, V. N.: Jet Separation in Conical Nozzles. J. Aeronaut. Soc., vol. 68, no. 648, Dec. 1964, pp. 808-817.

41. Kalt, Sherwin; and Badal, David L.: Conical Rocket Nozzle Performance Under Flow-Separated Conditions. J. Spacecr. & Rockets, vol. 2, no. 3, May-June 1965, pp. 447-449.

42. Lawrence, Roy A.: Symmetrical and Unsymmetrical Flow Separation in Supersonic Nozzles. Res. Rep. No. 67-1, Southern Methodist Univ. Inst. of Technol., Apr. 1967.

43. Grant, George K.: Flow Separation in Overexpanded Supersonic Nozzles. M.S. Thesis, Sacramento State Coll., May 25, 1967.

44. Grant, G. K.; and Hester, J. N.: Flow Separation in Overexpanded Supersonic Nozzles: A Boundary Layer Phenomena. 9th Liquid Propulsion Symposium, CPIA Pub. No. 155, Vol. 1 (Contract NOw 62-0604-c), Appl. Phys. Lab., Johns Hopkins Univ., Sept. 1967, pp. 445-464.

45. Zelenkov, O. S.; and Yurkov, A. V. (N. Alaechea, transl.): Experimental Study of Flow Separation in Overexpanded Conical Nozzles. FTD-HT-23-290-70, U.S. Air Force, July 1970. (Available from DDC as AD 712 943.)

46. Back, L. H.; Massier, P. F.; and Cuffel, R. F.: Heat-Transfer Measurements in the Shock-Induced Flow Separation Region in a Supersonic Nozzle. AIAA J., vol. 6, no. 5, May 1968, pp. 923-925.

47. Lawrence, Roy A.; and Weynand, Edmund E.: Factors Affecting Flow Separation in Contoured Supersonic Nozzles. AIAA J., vol. 6, no. 6, June 1968, pp. 1159-1160.

48. Miller, Eugene; and Migdal, David: Separation and Stability Studies of a Convergent-Divergent Nozzle. Rep. No. ADR 01-03-69.1, Grumman Aircraft Eng. Corp., Mar. 1969.

49. Miller, E. H.; and Migdal, D.: Separation and Stability Studies of a Convergent-Divergent Nozzle. J. Aircr., vol. 7, no. 2, Mar.-Apr. 1970, pp. 159-163.

50. Chapman, Dean R.; Kuehn, Donald M.; and Larson, Howard K.: Investigation of Separated Flows in Supersonic and Subsonic Streams With Emphasis on the Effect of Transition. NACA Rep. 1356, 1958.

51. Reshotko, Eli; and Tucker, Maurice: Effect of a Discontinuity on Turbulent Boundary-Layer-Thickness Parameters With Application to Shock-Induced Separation. NACA TN 3454, 1955.

52. Gadd, G. E.: Interactions Between Wholly Laminar or Wholly Turbulent Boundary Layers and Shock Waves Strong Enough To Cause Separation. J. Aeronaut. Sci., vol. 20, no. 11, Nov. 1953, pp. 729-739.

53. Sterrett, James R.; and Emery, James C.: Extension of Boundary-Layer-Separation Criteria to a Mach Number of 6.5 by Utilizing Flat Plates With Forward-Facing Steps. NASA TN D-618, 1960.

54. Holden, M. S.: Shock Wave-Turbulent Boundary Layer Interaction in Hypersonic Flow. AIAA Paper No. 72-74, Jan. 1972.

55. Mager, Artur: On the Model of the Free, Shock-Separated, Turbulent Boundary Layer. J. Aeronaut. Sci., vol. 23, no. 2, Feb. 1956, pp. 181-184.

56. Guman, William J.: On the Plateau and Peak Pressure of Regions of Pure Laminar and Fully Turbulent Separation in Two-Dimensional Supersonic Flow. J. Aero/Space Sci., vol. 26, no. 1, Jan. 1959, p. 56.

TABLE I.- DESCRIPTION OF NOZZLES AND TEST MEDIUMS

Symbol	Ref.	Nozzle type	α, deg, or M_e	γ	Reynolds number available	Test medium	Remarks
○	5	Conical	10, 15, 20, 30	1.2 to 1.25	No	RFNA-analine	
□	7	Conical	5, 15, 25, 35	1.4	Yes	Air	
◇	9	Conical	15	1.2	No	RFNA-analine	
△	11	2-D radial	15	1.4	Yes	Nitrogen	
◺	8	Conical	15	1.4	Yes	Air	
◺	12	Conical	$3\frac{1}{2}$, 6, 12	1.4	No	Air	
⬠	15	3-D contoured	----------	1.4	No	Air	Coflowing external stream
◇	17	Conical	$3\frac{1}{2}$, 6, 12, 25	1.4	No	Air	
◇	18	Conical	10, 15, 20	1.4	Yes	Air	
⬠	19	2-D radial	$2\frac{1}{2}$, 5, $7\frac{1}{2}$, $8\frac{1}{2}$, $12\frac{1}{2}$	1.4	Yes	Air	
▽	22	Conical	15	1.4	Yes	Air	Coflowing external stream
◁	24	Conical	15, 25, 29	1.4	No	Air	
◸	25	Conical	15	1.4	Yes	Air	
◸	25	3-D contoured	M_e = 5.02	1.4	Yes	Air	
⬠	26	Conical	7	1.4	No	Air	
⬠	27	3-D contoured	M_e = 2	1.4	Yes	Air	Coflowing external stream
⬠	28	3-D contoured	M_e = 3.4 to 5.7	1.4	No	Air	Ten different nozzles
⬠	28	Conical	15	1.4	No	Air	
◇	29	Conical	20, 25, 30	1.2	No	JP-4 oxygen	
◇	30	3-D contoured	----------	1.2	No	JP-4 oxygen	
▽	31	Conical	7, 15, 22	1.4	No	Air	
⬠	31	2-D radial	7, 15, 22	1.4	No	Air	
◹	33	3-D contoured	M_e = 4.6	1.3 to 1.4	No	Hydrazine; nitrogen	
◁	37	Conical	10	1.4	Yes	Air	Coflowing external stream
▷	38	Conical	10	1.4	No	Air	
◺	39	Conical	15	1.4	Yes	Air	
⬠	40	Conical	16, 17	1.2 to 1.3	No	85 to 87% HTP and kerosene	
⬠	41	Conical	15, $17\frac{1}{2}$	1.2	No	Nitroplasticized polyurethane and aluminum	
⊂	42	Conical	9, 15, 30	1.4	Yes	Air	
◁	42	3-D contoured	M_e = 4, 5	1.4	Yes	Air	
◁	42	2-D radial	10, 30	1.4	Yes	Air	
⬠	45	Conical	5, $7\frac{1}{2}$, 10, $12\frac{1}{2}$, 15	1.4	No	Air	
◇	46	Conical	15	1.4	Yes	Air	
◇	48	Conical	11.75	1.4	Yes	Air	

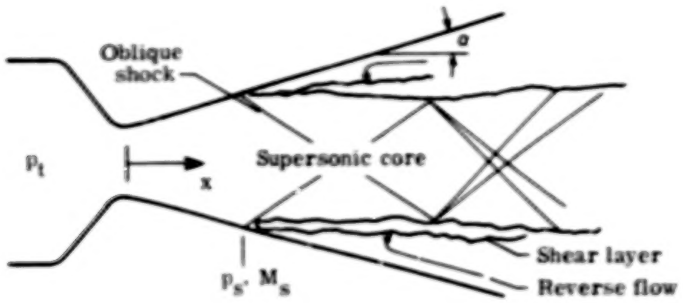

(a) Separation case. Viscid flow.

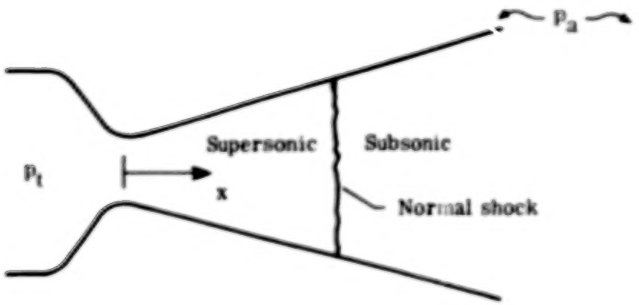

(b) Normal-shock case. Inviscid flow.

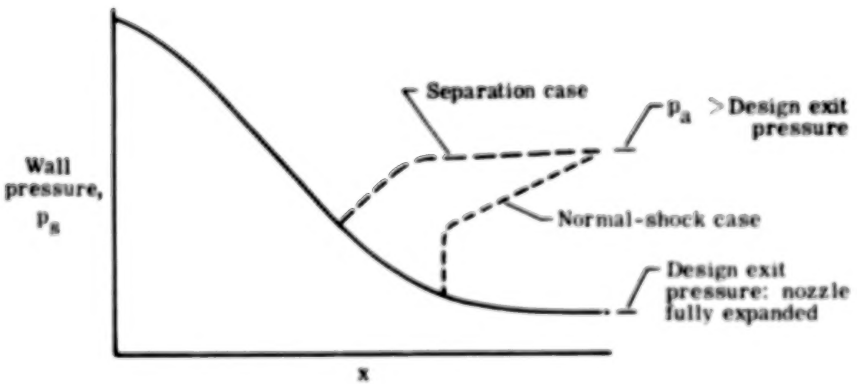

(c) Wall pressure distributions.

Figure 1.- Flow in overexpanded nozzles.

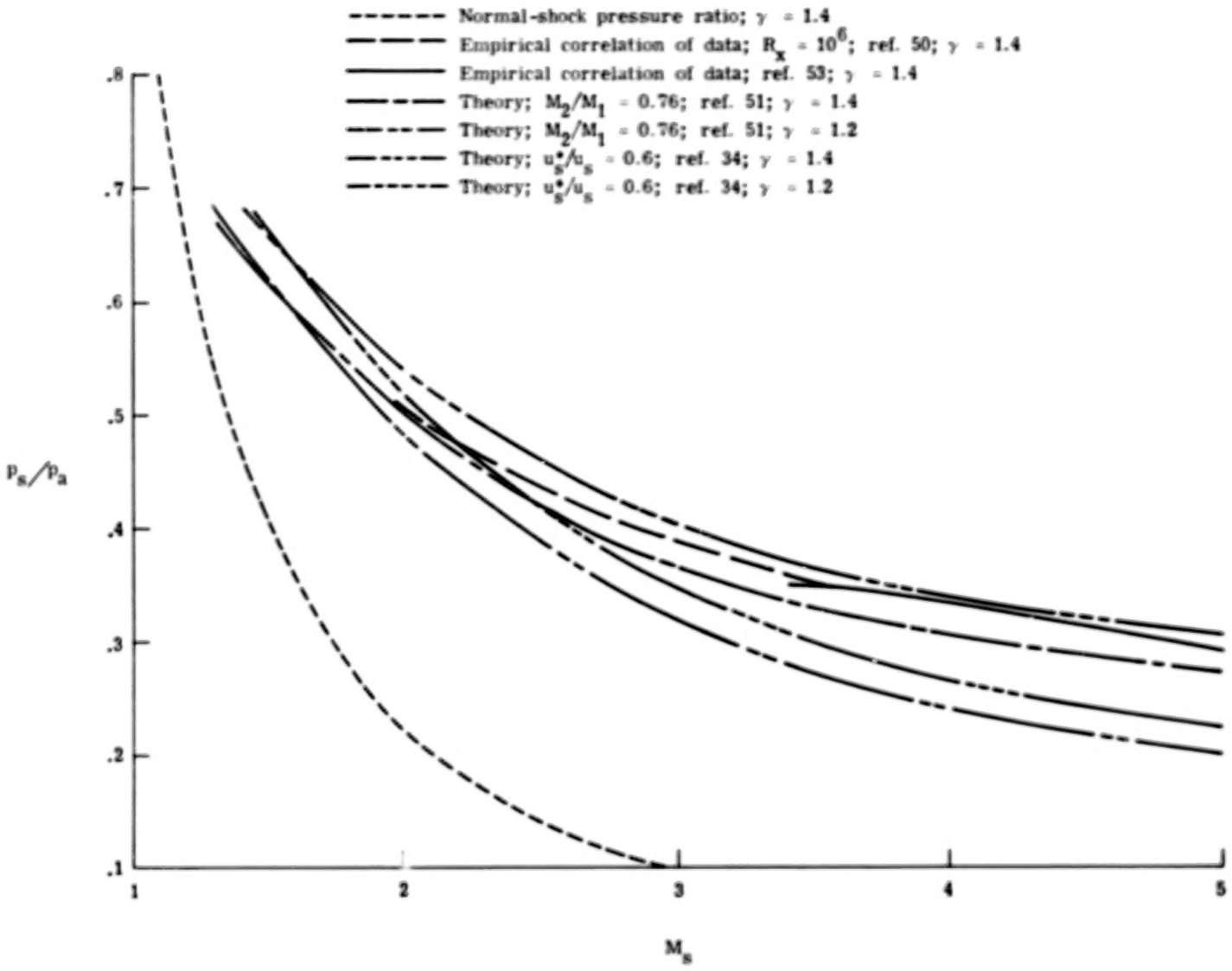

Figure 2.- Predictions of separation pressure ratio as a function of Mach number. Theories and correlations of zero-pressure-gradient experimental data.

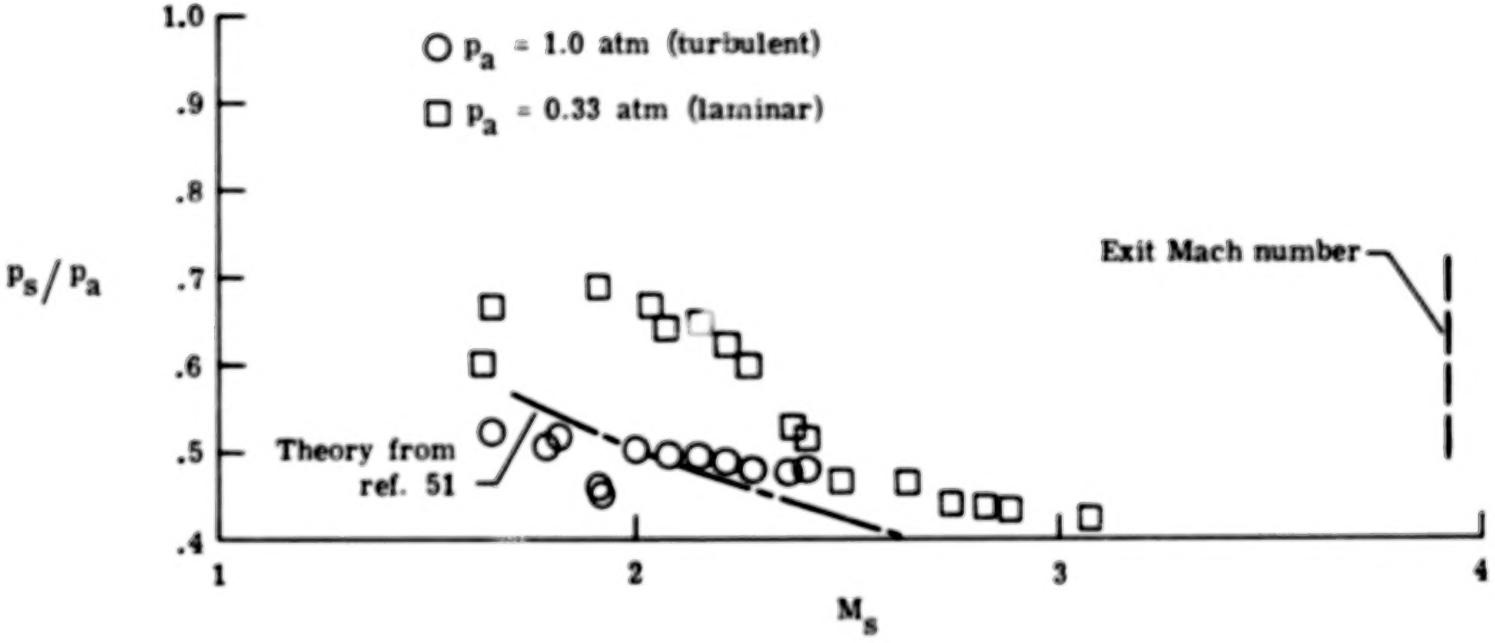

(a) Data from reference 8; ambient pressure varied; conical nozzle ($\alpha = 15^{o}$).

Figure 3.- Typical examples of laminar and turbulent separation pressure ratios as a function of separation Mach number.

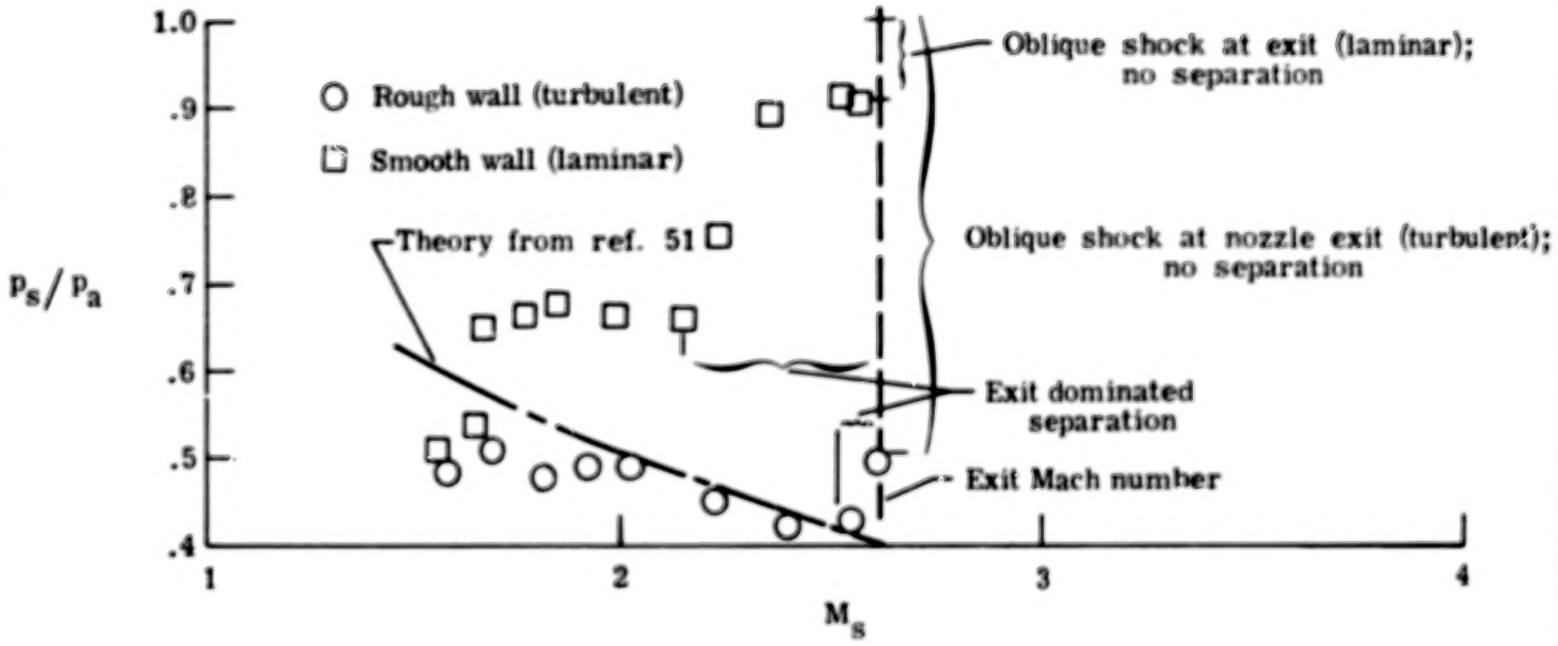

(b) Data from reference 38; smooth and rough wall; conical nozzle ($\alpha = 10^{o}$). p_a = Constant = 1.0 atm.

Figure 3.- Concluded.

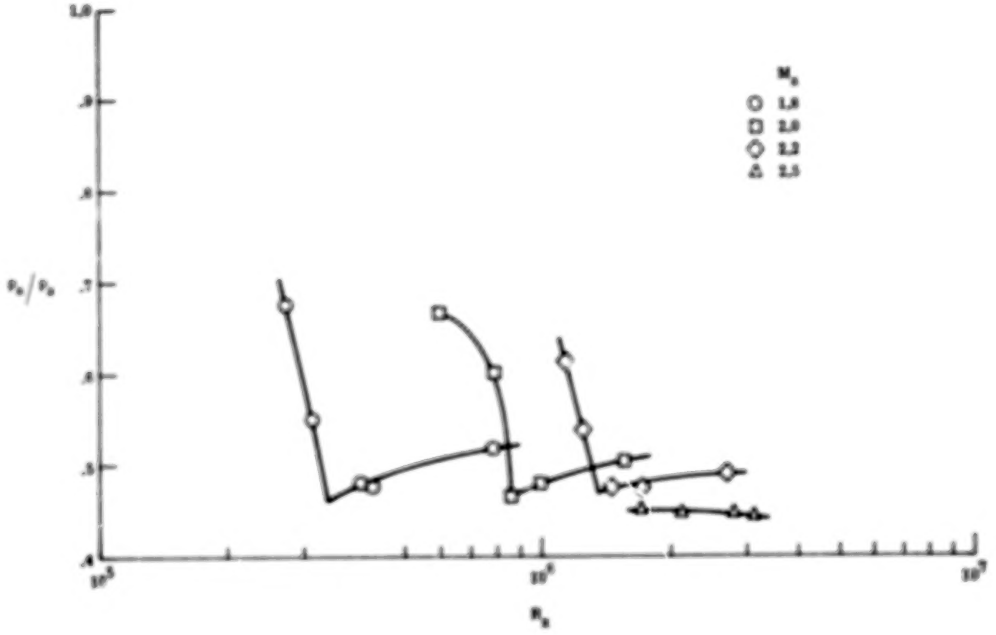

(a) Length Reynolds number.

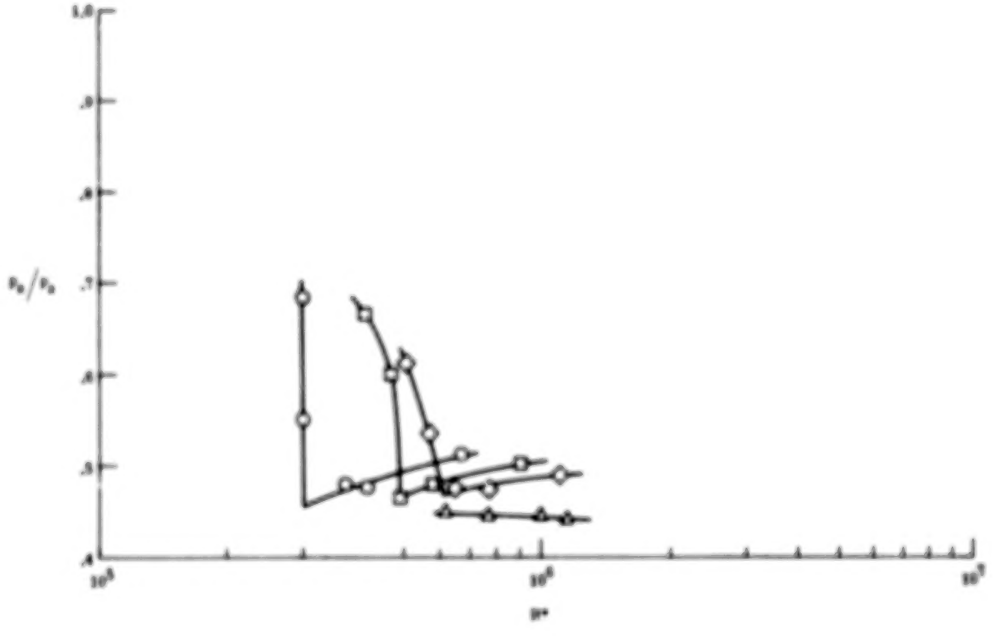

(b) Nozzle-throat Reynolds number.

Figure 4.- Separation pressure ratio as a function of separation Reynolds number. Data from reference 8.

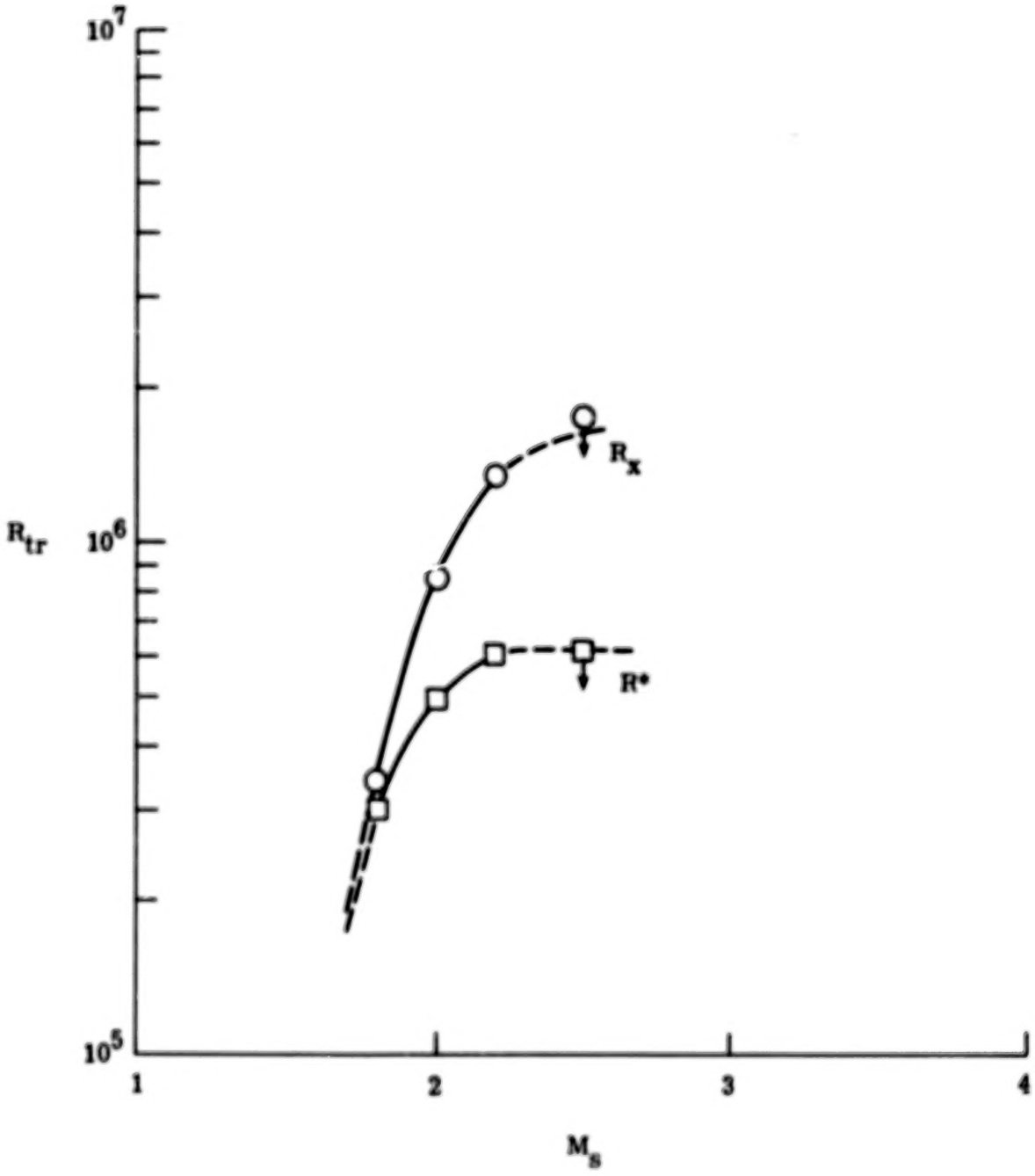

Figure 5.- Nozzle transition Reynolds numbers from data of figure 4.

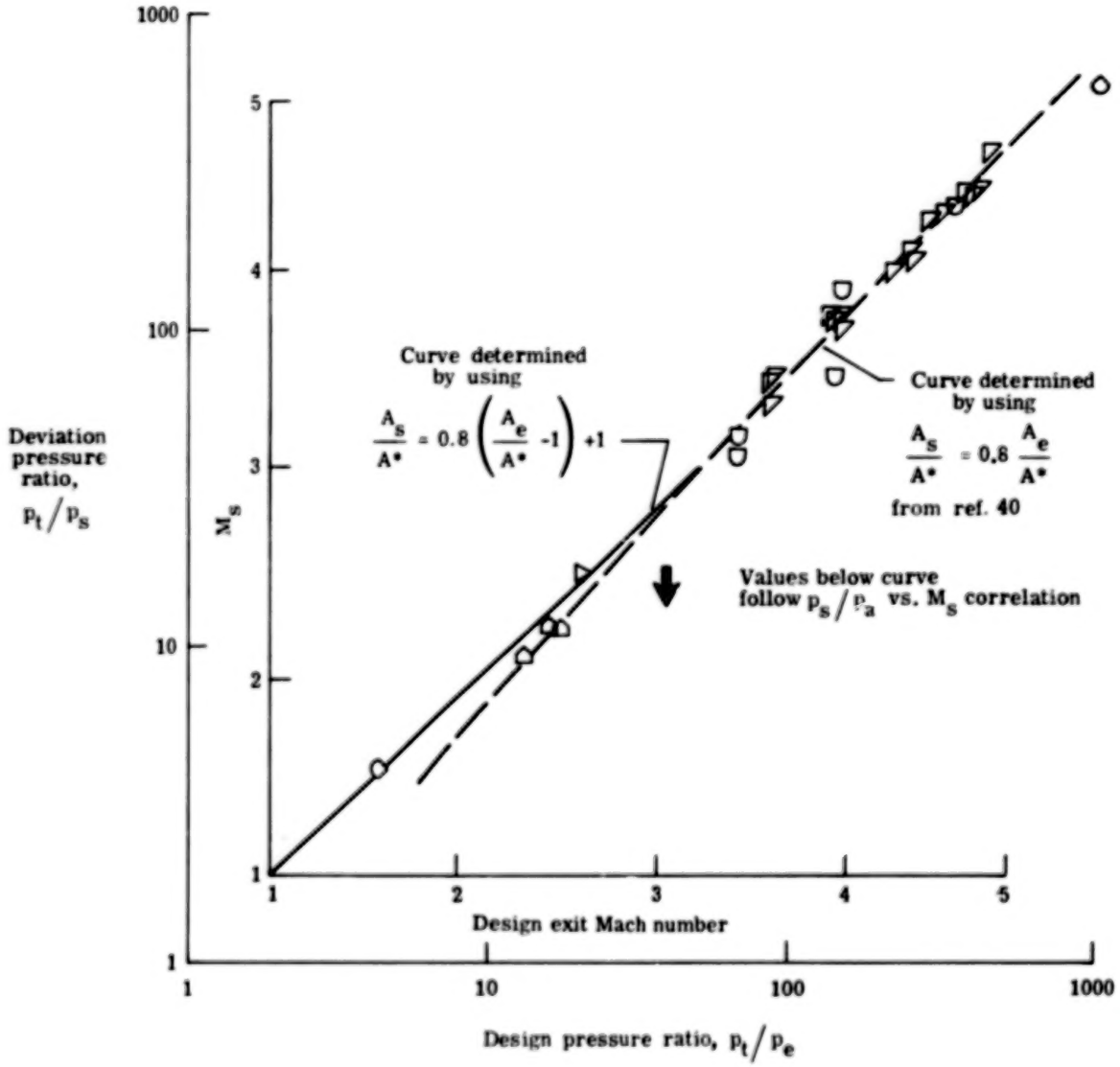

Figure 6.- Pressure ratio at which turbulent separation pressure ratio p_s/p_a deviates from correlation. Mach number is calculated for $\gamma = 1.4$. For symbol key see table I.

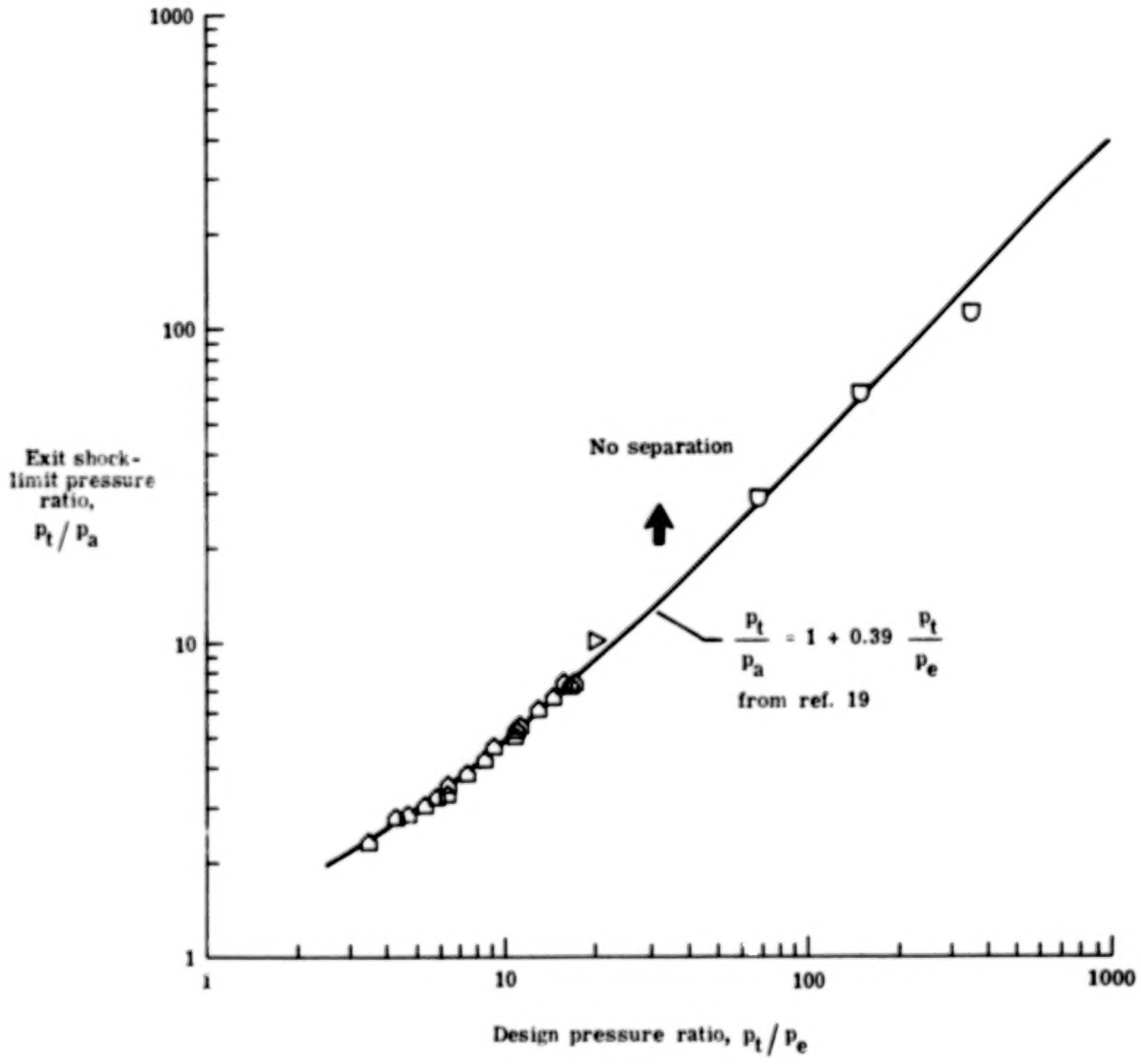

Figure 7.- Minimum nozzle pressure ratio p_t/p_a for which the oblique shock remains at exit and flow does not separate. Turbulent flow. For symbol key see table I.

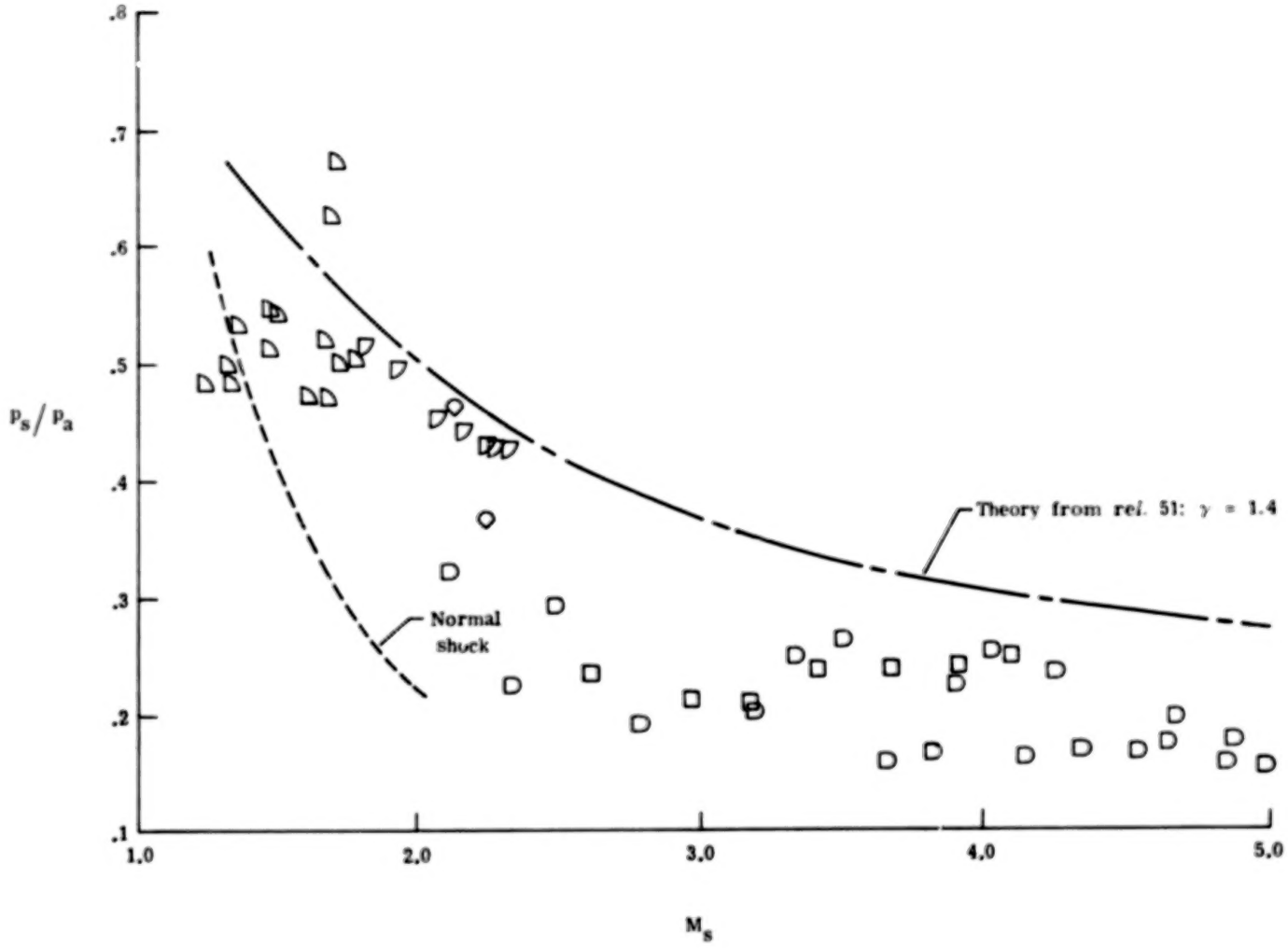

(a) Conical nozzles. $\alpha = 3\frac{1}{2}^\circ$ to $7\frac{1}{2}^\circ$.

Figure 8.- Separation pressure ratio as a function of separation Mach number. For symbol key see table I. Solid symbols denote laminar data as defined in figure 5.

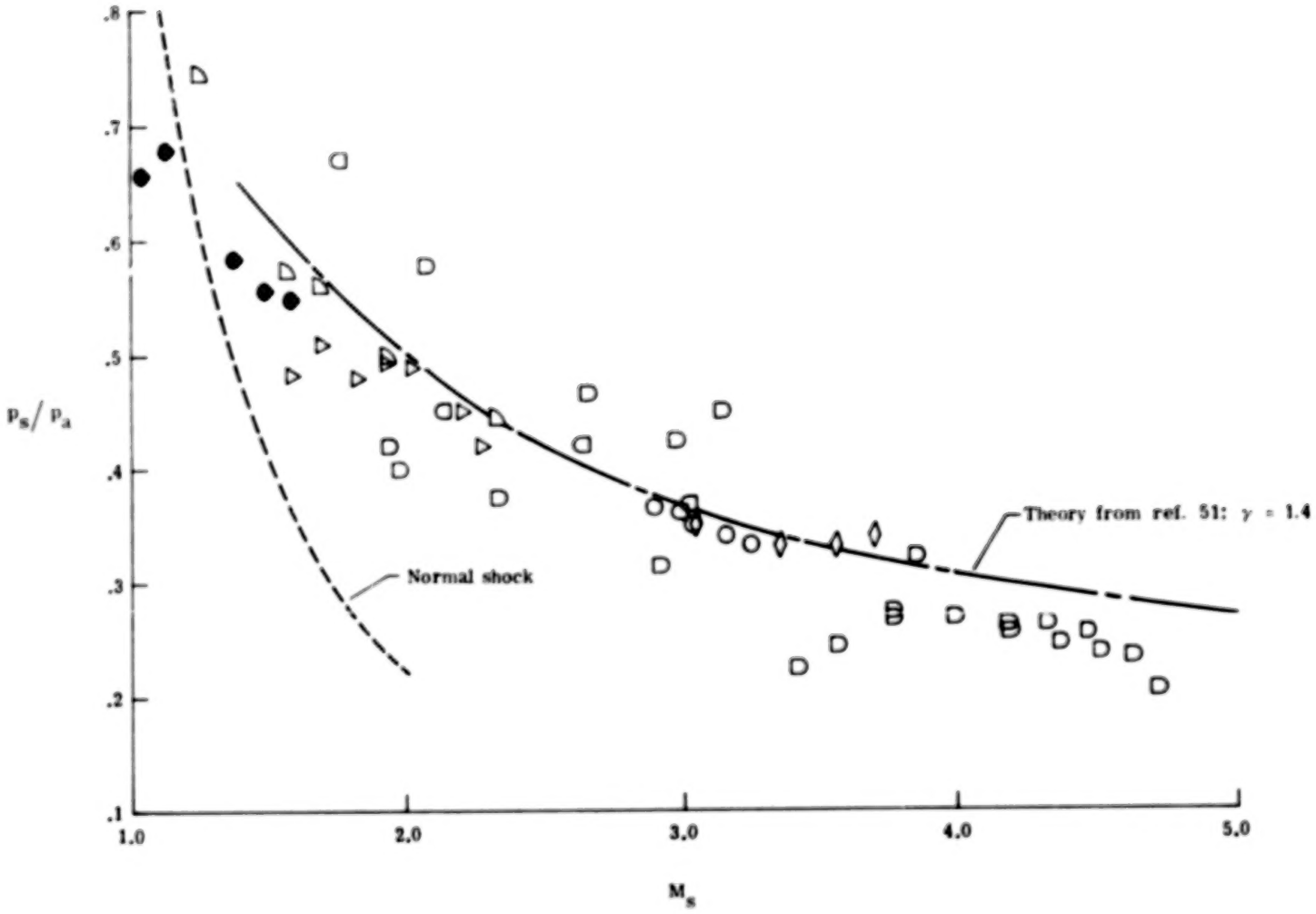

(b) Conical nozzles. $\alpha = 9^o$ to $12\frac{1}{2}^o$.

Figure 8.- Continued.

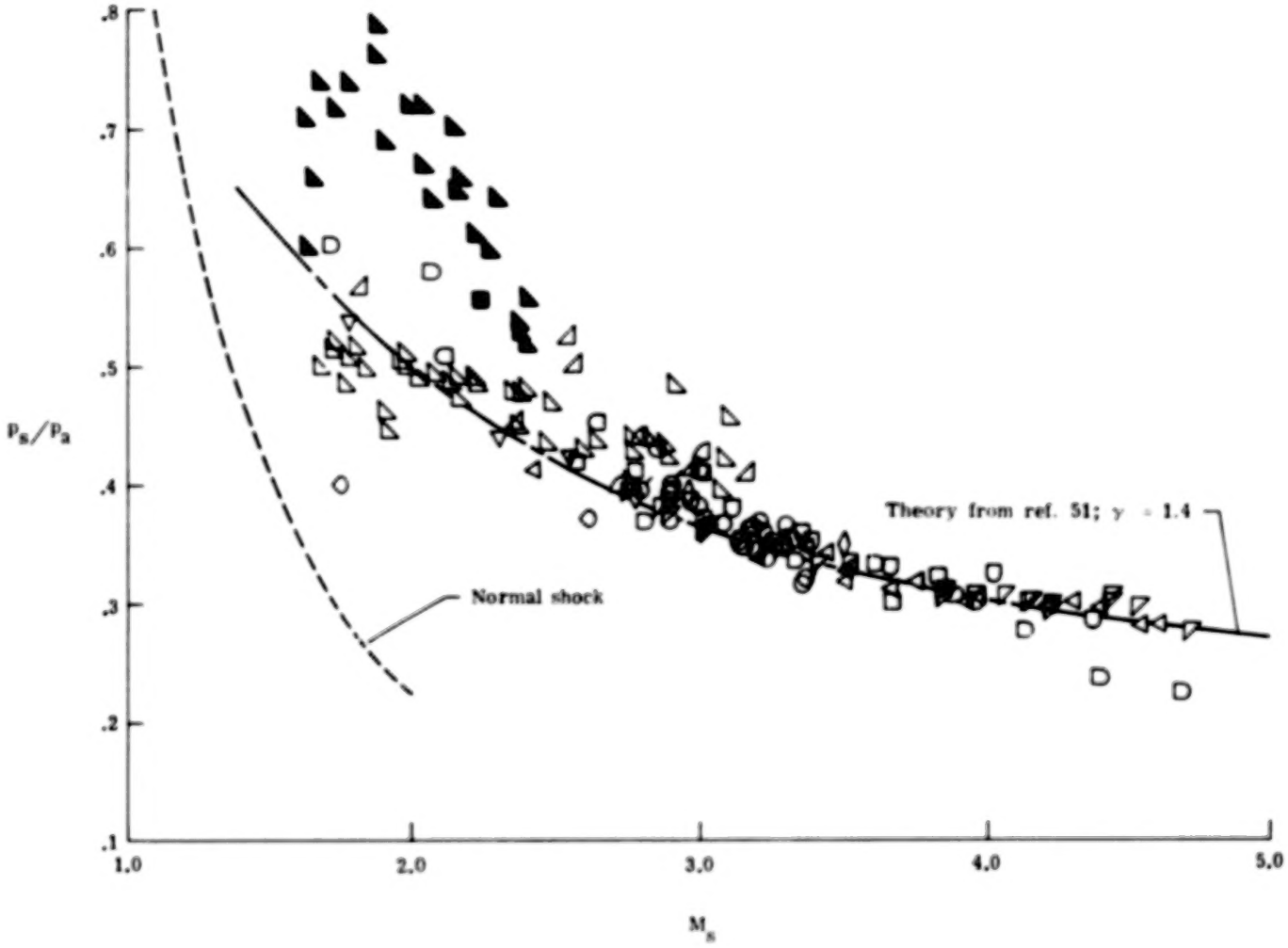

(c) Conical nozzles. $\alpha = 15^{o}$.

Figure 8.- Continued.

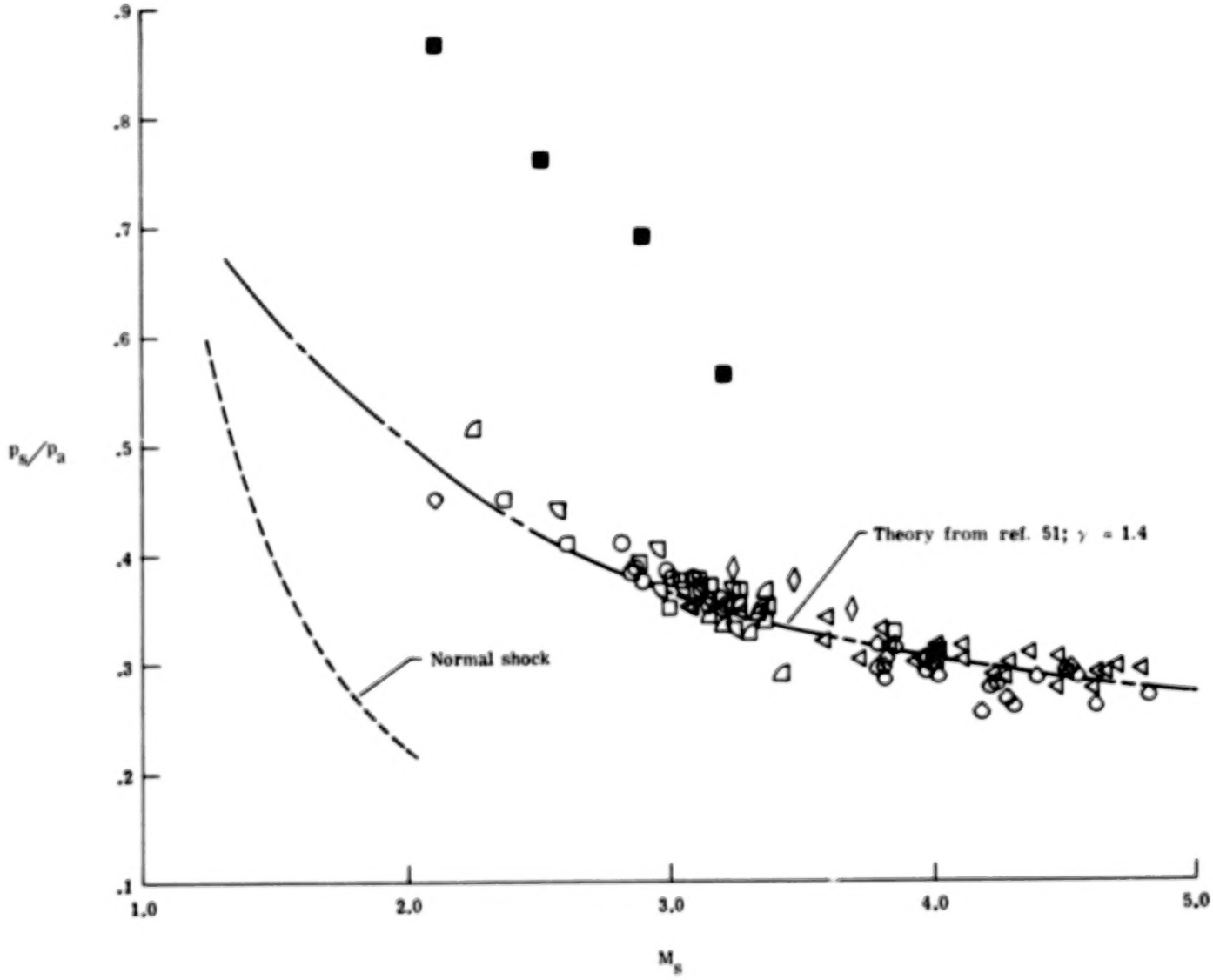

(d) Conical nozzles. $\alpha = 16^{o}$ to 35^{o}.

Figure 8.- Concluded.

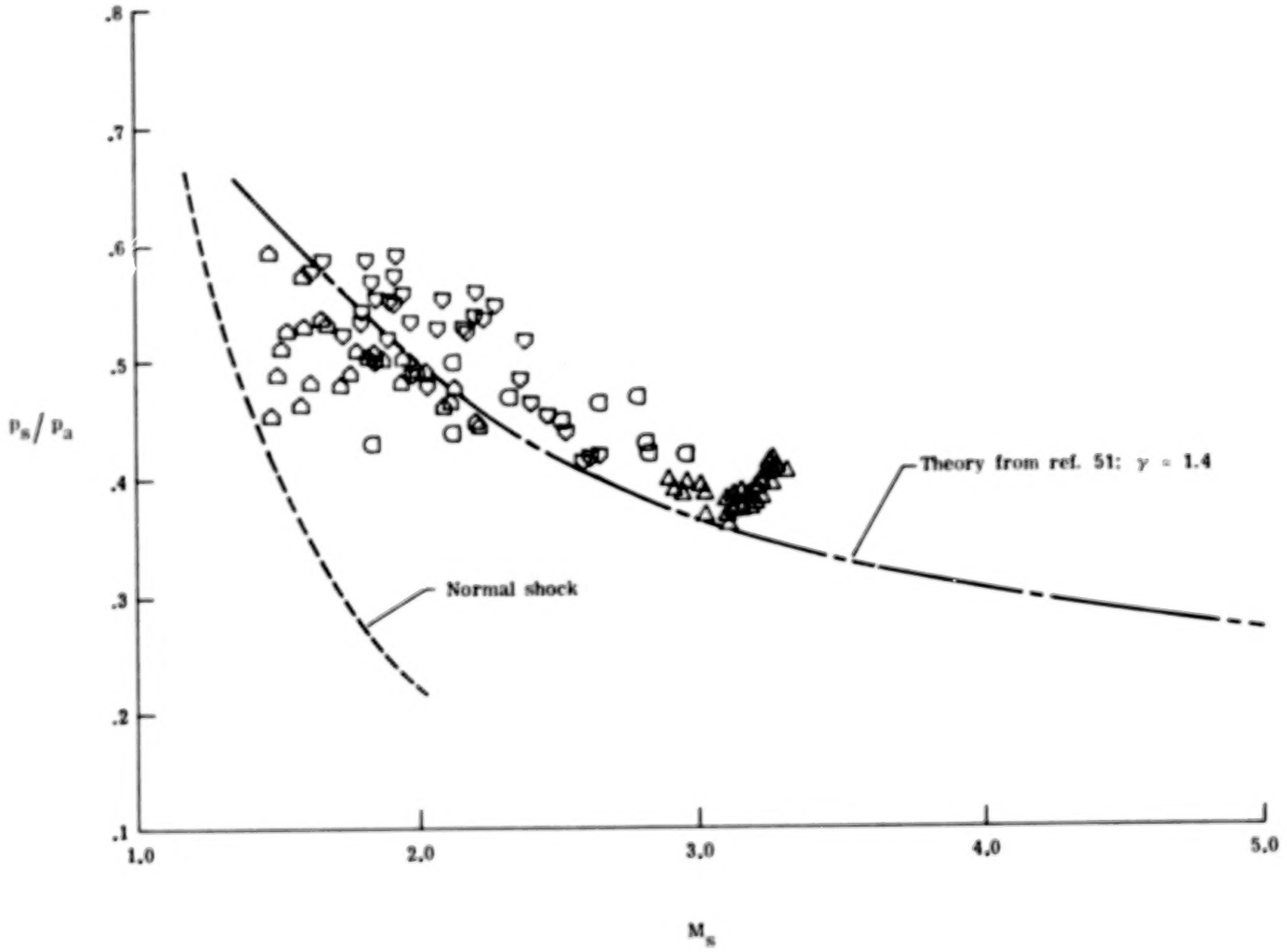

Figure 9.- Separation pressure ratio as a function of separation Mach number for two-dimensional wedge-flow nozzles. $\alpha = 2\frac{1}{2}^{\circ}$ to 30°. For symbol key see table I.

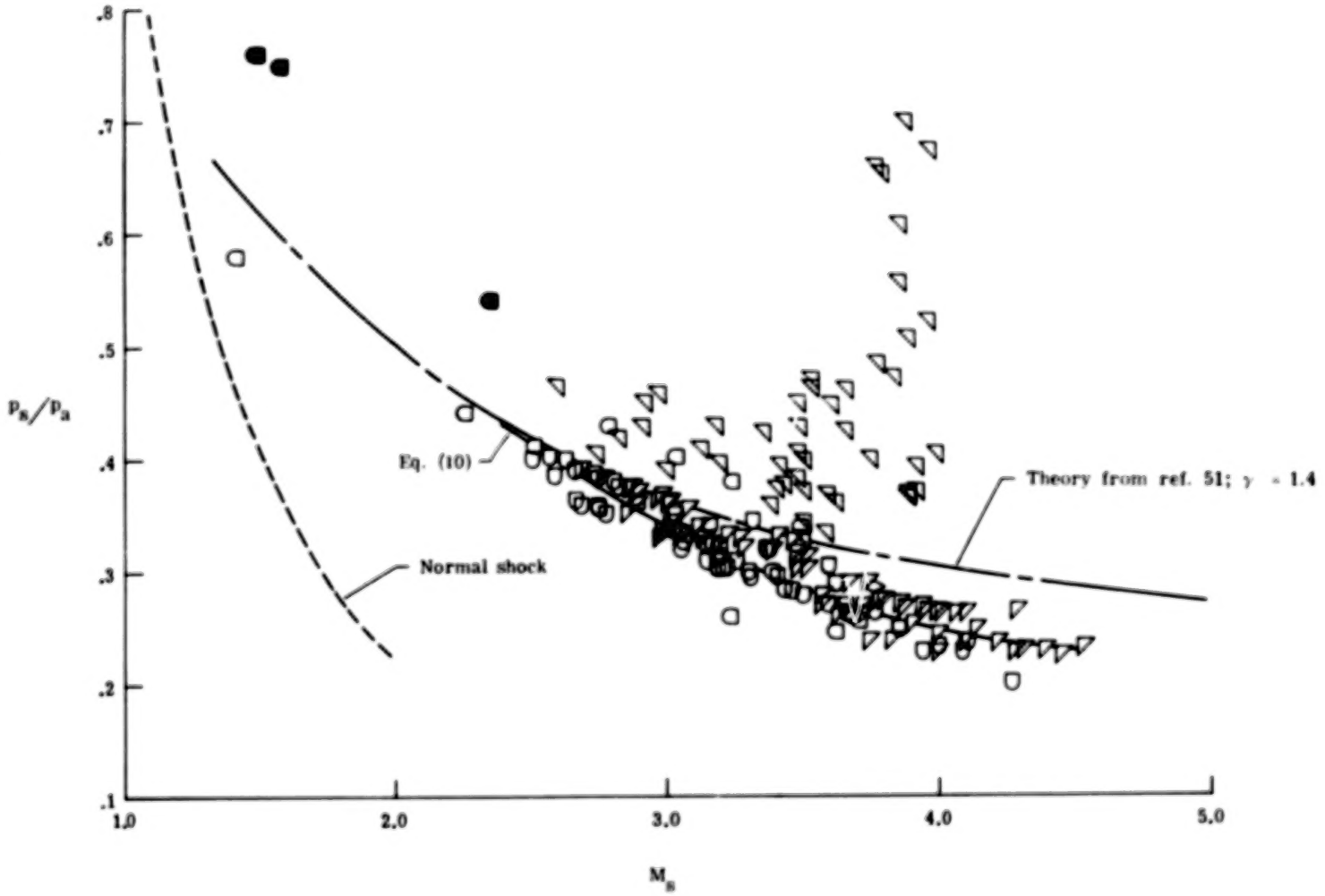

Figure 10.- Separation pressure ratio as a function of separation Mach number for axisymmetrical contoured nozzles. For symbol key see table I. Solid symbols denote laminar data as defined in figure 5.

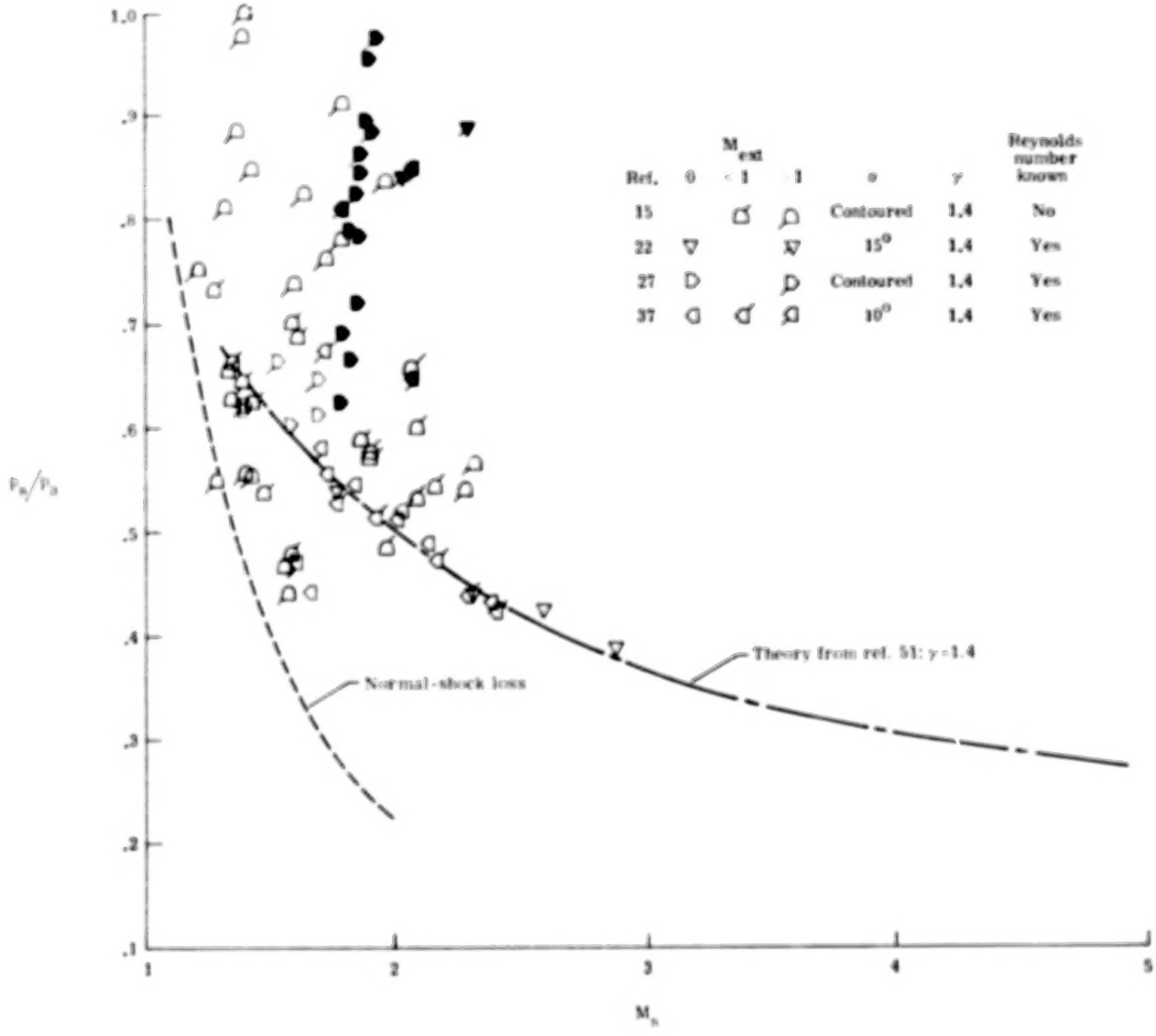

Figure 11.- Separation pressure ratio as a function of separation Mach number for tests with a coflowing external stream. Solid symbols denote laminar data as defined in figure 5.

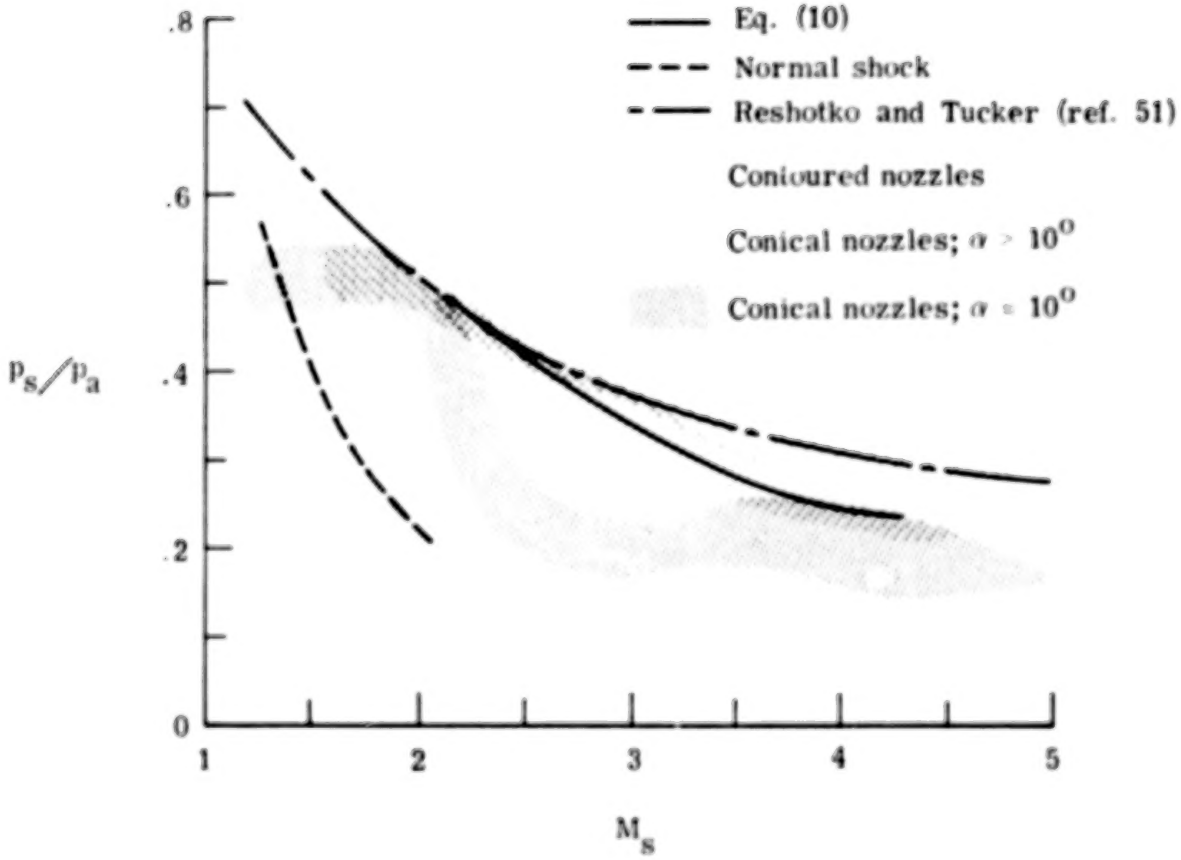

Figure 12.- Summary plot of separation pressure ratios as a function of separation Mach number.

1 Report No. NASA TP-1207	2 Government Accession No.	3 Recipient's Catalog No.
4 Title and Subtitle: TURBULENT-FLOW SEPARATION CRITERIA FOR OVEREXPANDED SUPERSONIC NOZZLES		5 Report Date: August 1978 6 Performing Organization Code:
7 Author(s): E. Leon Morrisette and Theodore J. Goldberg		8 Performing Organization Report No.: L-11530 10 Work Unit No.: 505-06-15-01
9 Performing Organization Name and Address: NASA Langley Research Center, Hampton, VA 23665		11 Contract or Grant No.: 13 Type of Report and Period Covered: Technical Paper
12 Sponsoring Agency Name and Address: National Aeronautics and Space Administration, Washington, DC 20546		14 Sponsoring Agency Code:

15 Supplementary Notes:

16 Abstract:

A comprehensive compilation of available turbulent-flow separation data for overexpanded supersonic nozzles is presented with a discussion of correlation techniques and prediction methods. Data are grouped by nozzle types: conical, contoured, and two-dimensional wedge. Correlation of conical-nozzle separation is found to be independent of nozzle divergence half-angle above about 9°, whereas the contoured-nozzle data follow a different correlation curve. Zero-pressure-gradient prediction techniques are shown to predict adequately the higher divergence-angle conical separation data, and an empirical equation is given for the contoured-nozzle data correlation. Flow conditions for which the correlations are invalid are discussed and bounded. A nozzle boundary-layer transition criterion is presented which can be used to show that much of the noncorrelating data in the literature are concerned with nonturbulent separation and which explains the previously reported "external flow effects" on nozzle separation.

17 Key Words (Suggested by Author(s))	18 Distribution Statement
Flow separation Turbulent boundary layer Supersonic nozzle flow	Unclassified – Unlimited Subject Category 34

19 Security Classif. (of this report)	20 Security Classif. (of this page)	21 No. of Pages	22 Price*
Unclassified	Unclassified	36	$4.50

*For sale by the National Technical Information Service, Springfield, Virginia 22161

NASA-Langley, 1978

37